PB84-113752

Effects of Photochemical Kinetic Mechanisms on Oxidant Model Predictions

Systems Applications, Inc., San Rafael, CA

Prepared for

Environmental Sciences Research Lab.
Research Triangle Park, NC

Nov 83

U.S. Department of Commerce
National Technical Information Service
NTIS

BEGIN FIRST LINE OF TEXT HERE
TYPING GUIDE SHEET
CENTER OF PAGE
TOP OF IMAGE AREA
DROPPED HEAD; BEGIN SECTIONS HERE
6-1/2"
9-1/8"
BEGIN LAST LINE OF TEXT
3/8"
BOTTOM OF IMAGE AREA, OUTSIDE DIMENSION FOR TABLES AND ILLUSTRATIONS
PAGE NUMBER
EPA-287 (Cin.)
(4-76)

PB84-113752
EPA-600/3-83-111
November 1983

EFFECTS OF PHOTOCHEMICAL KINETIC MECHANISMS ON OXIDANT MODEL PREDICTIONS

by

J. P. Killus
G. Z. Whitten

Systems Applications, Inc.
101 Lucas Valley Road
San Rafael, California 94903

P.O. No. 2D5537NASA

Project Officer

Marcia C. Dodge
Atmospheric Chemistry and Physics Division
Environmental Sciences Research Laboratory
Research Triangle Park, North Carolina 27711

ENVIRONMENTAL SCIENCES RESEARCH LABORATORY
OFFICE OF RESEARCH AND DEVELOPMENT
U.S. ENVIRONMENTAL PROTECTION AGENCY
RESEARCH TRIANGLE PARK, NORTH CAROLINA 27711

REPRODUCED BY
NATIONAL TECHNICAL
INFORMATION SERVICE
U.S. DEPARTMENT OF COMMERCE
SPRINGFIELD, VA. 22161

TECHNICAL REPORT DATA
(Please read Instructions on the reverse before completing)

1. REPORT NO.	2.	3. RECIPIENT'S ACCESSION NO.
EPA-600/3-83-111		PB84 113752

4. TITLE AND SUBTITLE	5. REPORT DATE
EFFECTS OF PHOTOCHEMICAL KINETIC MECHANISMS ON OXIDANT MODEL PREDICTIONS	November 1983
	6. PERFORMING ORGANIZATION CODE
7. AUTHOR(S)	8. PERFORMING ORGANIZATION REPORT NO.
J. P. Killus and G. Z. Whitten	
9. PERFORMING ORGANIZATION NAME AND ADDRESS	10. PROGRAM ELEMENT NO.
Systems Applications, Inc. 101 Lucas Valley Road San Rafael, CA 94903	CDWA1A/01-3052 (FY-83)
	11. CONTRACT/GRANT NO.
	Purchase Order 2D5537NASA
12. SPONSORING AGENCY NAME AND ADDRESS	13. TYPE OF REPORT AND PERIOD COVERED
Environmental Sciences Research Laboratory-RTP, NC Office of Research and Development U.S. Environmental Protection Agency Research Triangle Park, NC 27711	Final Report (9/82 - 6/83)
	14. SPONSORING AGENCY CODE
	EPA/600/09

15. SUPPLEMENTARY NOTES

16. ABSTRACT

The comparative effects of kinetic mechanisms on oxidant model predictions have been tested using two different mechanisms [the Carbon-Bond Mechanism II (CBM-II) and the Demerjian Photochemical Box Model (DPBM) mechanism] in three air quality models [the OZIPM/EKMA, the Urban Airshed Model (UAM), and a trajectory model with the same inputs and chemistry as the UAM]. Simulations were performed for Los Angeles using a 1974 base case and a 1987 emission inventory (reflecting controls). The two kinetic mechanisms produced different results. Although the DPBM mechanism produced results similar to those for the CBM-II with the 1974 base case for all three models, it exhibited a greater response to the 1987 control scenario (predicting less ozone). In simulations employing the CBM-II, the ozone reductions predicted using the 1987 emission inventory were 31, 34, and 33 % for the UAM, trajectory model, and OZIPM/EKMA, respectively. The ozone reductions predicted by the UAM trajectory model and OZIPM/EKMA for the 1987 inventory simulations employing the DPBM were 41, 51, and 53 %, respectively. Also, reduction of peak ozone anywhere in the UAM simulation grid was 26 % for the CBM-II/Airshed simulations and 40 % for the DPBM/Airshed simulations.

17. KEY WORDS AND DOCUMENT ANALYSIS

a. DESCRIPTORS	b. IDENTIFIERS/OPEN ENDED TERMS	c. COSATI Field/Group

18. DISTRIBUTION STATEMENT	19. SECURITY CLASS *(This Report)*	21. NO. OF PAGES
RELEASE TO PUBLIC	UNCLASSIFIED	60
	20. SECURITY CLASS *(This page)*	22. PRICE
	UNCLASSIFIED	

EPA Form 2220-1 (Rev. 4-77) PREVIOUS EDITION IS OBSOLETE

NOTICE

This document has been reviewed in accordance with U.S. Environmental Protection Agency policy and approved for publication. Mention of trade names or commercial products does not constitute endorsement or recommendation for use.

BEGIN FIRST LINE OF TEXT HERE
TYPING GUIDE SHEET
CENTER OF PAGE
TOP OF IMAGE AREA
DROPPED HEAD; BEGIN SECTIONS HERE

ABSTRACT

The comparative effects of kinetic mechanisms on oxidant model predictions have been tested using two different mechanisms--the Carbon-Bond Mechanism II (CBM-II) and the Demerjian Photochemical Box Model (DPBM) Mechanism--in conjunction with three air quality models--OZIPM/EKMA, the Urban Airshed Model (UAM), and a trajectory model with the same inputs and chemistry as the UAM. Simulations were performed for the Los Angeles Airshed using a 1974 base case and a 1987 emission inventory (reflecting controls).

To achieve agreement in absolute predictions among the three models, it was necessary to treat two significant processes in the OZIPM/EKMA simulations: surface deposition and the photochemical reaction of material aloft before entrainment by the growing mixed layer. These two processes are not normally modeled in OZIPM/EKMA and could be treated only in a general, averaged fashion. With this treatment, however, results for the three models were within 25 percent overall agreement and within 10 percent agreement for the peak value when the same kinetic mechanism was used.

The two kinetic mechanisms produced different results. Although the DPBM Mechanism gave results similar to the CBM-II with the 1974 base case for all three models, it exhibited a greater response to the 1987 control scenario (predicting less ozone). For CBM-II simulations, the ozone reduction for the 1987 emissions case was 31, 34, and 33 percent for the UAM, trajectory model, and OZIPM/EKMA, respectively. The ozone reduction for the DPBM Mechanism with 1987 emissions was 41, 51, and 53 percent, respectively. Also, reduction of peak ozone anywhere in the Urban Airshed simulation grid was 26 percent for the CBM-II/Airshed simulations and 40 percent for the DPBM/Airshed simulations.

The greater response to hydrocarbon control exhibited by the DPBM Mechanism compared to that of the CBM-II is contrary to the findings of Jeffries et al., 1981, which indicated a greater response to control for the CBM-II than for the DPBM. However, the study of Jeffries et al. examined uniform control of hydrocarbons, whereas the 1987 emission inventory used in this study was a realistic control scenario that included the effects of population growth and differing controls on various source categories. These factors resulted in a shift in hydrocarbon speciation, most notably a decrease in olefins relative to other hydrocarbons. The DPBM Mechanism demonstrated an overresponse to the olefin component of the hydrocarbon mix. Thus, the difference in the models' response to the control strategy was traced to a specific feature of the DPBM Mechanism.

BEGIN LAST LINE OF TEXT
BOTTOM OF IMAGE AREA; OUTSIDE DIMENSION FOR TABLES AND ILLUSTRATIONS
PAGE NUMBER
EPA-287 (Cin.) (4-76)

BEGIN FIRST LINE OF TEXT HERE
TYPING GUIDE SHEET
CENTER OF PAGE
TOP OF IMAGE AREA
DROPPED HEAD; BEGIN SECTIONS HERE

CONTENTS

Abstract..... iii
Figures..... vi
Tables..... vii
1. Introduction..... 1
2. Airshed Model Calculations Obtained Using the DPBM Mechanism..... 5
Results of the Base-Case Airshed Model Simulation Using the DPBM Mechanism..... 7
3. Comparisons of the Results of Simple and Complex Trajectory Models with Airshed Model Results..... 25
Comparison of the ACTM and Airshed Models..... 25
The OZIPM/EKMA Model..... 29
4. Results and Discussion..... 34
Summary and Conclusions..... 37
References..... 38

Appendix
A. CHEM Routine for DPBM Mechanism, Including Steady-State Relationships..... 41
B. Tests of the Demerjian Photochemical Box Model (DPBM) Mechanism using Smog Chamber Data..... 46

BEGIN LAST LINE OF TEXT
BOTTOM OF IMAGE AREA, OUTSIDE DIMENSION FOR TABLES AND ILLUSTRATIONS
3/8"

EPA-287 (Cin.)
(4-76)

BEGIN FIRST LINE OF TEXT HERE
TYPING GUIDE SHEET
CENTER OF PAGE
TOP OF IMAGE AREA
DROPPED HEAD; BEGIN SECTIONS HERE

FIGURES

Number		Page
1	Control Predictions for Three NO_x Control Conditions by Method/Day/Mechanism.....	3
2	Comparison of O_3 Results for Los Angeles, 27 June 1974, (Airshed Base Case) for the DPBM Mechanism and CBM-II.....	8
3	Comparison of O_3 Results for Los Angeles, 27 June 1987, for the DPBM Mechanism and the CBM-II.....	16
4	Trajectory of Air Parcel on 27 June 1974 at 0500 - 1700.....	26
5	Comparison of Model Results for the CBM-II Simulations.....	27
6	Comparison of Model Results for the DPBM Mechanism Simulations.....	28
7	Comparison of Model Results Showing Effects of Model Subcomponents.....	31

6-1/2"
BEGIN LAST LINE OF TEXT
BOTTOM OF IMAGE AREA, OUTSIDE DIMENSION FOR TABLES AND ILLUSTRATIONS
3/8"

EPA-287 (Cir.)
(4-76)

BEGIN FIRST LINE OF TEXT HERE
TYPING GUIDE SHEET
CENTER OF PAGE
TOP OF IMAGE AREA
DROPPED HEAD; BEGIN SECTIONS HERE

TABLES

Number		Page
1	The Demerjian Photochemical Box Model Mechanism.....	6
2	Carbon Numbers for Species in CBM and DPBM.....	7
3	Airshed Results for 1974 and 1987 Scenarios.....	15
4	Emission Inventory Information.....	23
5	Comparison of OZIPM and ACTM Trajectory Models.....	30
6	Loss Rates of Chemical Species through Deposition for ACTM (Fontana Trajectory for CBM Simulation).....	33
7	A Comparison of ACTM, Airshed, and OZIPM/EKMA Model Results for the Fontana Trajectory Using the DPBM and Carbon-Bond Mechanisms.....	35
8	Effect of Controls on ACTM, Airshed, and OZIPM/EKMA Model Predictions for the Fontana Trajectory.....	36

BEGIN LAST LINE OF TEXT
3/8"
BOTTOM OF IMAGE AREA; OUTSIDE DIMENSION FOR TABLES AND ILLUSTRATIONS

EPA-287 (Cin.)
(4-76)

BEGIN FIRST LINE OF TEXT HERE
TYPING GUIDE SHEET
CENTER OF PAGE
TOP OF IMAGE AREA
DROPPED HEAD; BEGIN SECTIONS HERE

SECTION 1

INTRODUCTION

The control of urban photochemical smog through the reduction of smog precursors (reactive organics and nitrogen oxides) is an established regulatory practice. Because photochemical oxidants are secondary products of reactive precursors whose chemical reactions are often highly nonlinear, there exists no simple methodology for accurately predicting the effects of reducing precursor emissions on smog formation. Available models that attempt to predict those effects include highly sophisticated, grid-based, reactive dispersion models (e.g., Reynolds, 1977; MacCracken and Sauter 1975; McRae et al. 1982), multilayer trajectory models (Lurman et al. 1979; Reynolds et al. 1979) and various one-dimensional "box" models, both moving and stationary.

Photochemical box models can be exercised at different levels of sophistication, and their outputs can be interpreted in various ways. Demerjian and Schere (1979) have reported the application of a sophisticated photochemical box model to Houston, Texas, and Brice (1983) has reported the application of a box model to the United Kingdom. For simple box model applications, the computer program OZIPP (and OZIPM), which was developed as part of the EPA Empirical Kinetic Modeling Approach (EKMA), can also be used. Conceptually, EKMA is based on a Lagrangian, or moving, box model approach to photochemical air quality analysis.

In the EKMA methodology, multiple simulations are used to construct a series of ozone isopleths as a function of initial precursors (hydrocarbons and nitrogen oxides). Control requirements are then obtained graphically from the isopleth diagram by assuming that precursor concentrations are linearly related to emissions. The simulations on which the isopleths are based can be performed at two different levels of detail: Level II, which requires a detailed meteorological description of the air parcel trajectory and gridded emissions along that trajectory, and Level III, which makes standard assumptions about the meteorology and which uses a county-wide average for the emissions rates.

Jeffries et al. (1981) recently conducted a study to assess the effect of using different chemical mechanisms on oxidant control strategies predicted

BEGIN LAST LINE OF TEXT
BOTTOM OF IMAGE AREA, OUTSIDE DIMENSION FOR TABLES AND ILLUSTRATIONS
3/8"

PAGE NUMBER
EPA-287 (Cin.)
(4-76)

BEGIN FIRST LINE OF TEXT HERE
TYPING GUIDE SHEET
CENTER OF PAGE
TOP OF IMAGE AREA
DROPPED HEAD: BEGIN SECTIONS HERE

with the EKMA procedure. Four kinetic mechanisms were investigated in this study: CBM-II (Whitten et al., 1980), Dodge (1977), CIT (Falls and Seinfeld, 1978), and the Demerjian Photochemical Box Model Mechanism (DPBM) (Demerjian and Schere, 1979). The performance of each mechanism was first evaluated using smog chamber data of irradiated auto exhaust and NO_x mixtures. All mechanisms except the CIT mechanism were able to reproduce the chamber observations within the range of experimental error. The three mechanisms that were able to reproduce the data (Dodge, CBM-II, and DPBM) were then used in EKMA Level II and Level III analyses with the St. Louis RAPS data base. For each of the days modeled in this study, O_3 isopleths were generated and the hydrocarbon control estimates needed to achieve the ozone air quality standard were calculated.

Jeffries et al. (1981) found that the most important factor in control effectiveness for the Level II EKMA methodology was the choice of day. The day requiring the most hydrocarbon control to meet the NAAQS of 0.12 ppm ozone was not the day exhibiting the maximum ozone value, but the day exhibiting the maximum ozone value aloft. Obviously, the greater the background ozone (which is presumed uncontrollable), the more stringent the control requirements. This is probably true for background hydrocarbons as well, though Jeffries et al. did not address this issue.

9-1/8"

The second most important factor was found to be the choice of a kinetic mechanism. As shown in Figure 1, the hydrocarbon control strategy estimates differed greatly, depending on which of the three mechanisms was used. The results of Jeffries et al. (1981) clearly demonstrate that the choice of chemical mechanisms can have a substantial impact on predictions of control strategies when used in a simple model such as EKMA. The objective of this study was to determine if the choice of chemical mechanisms also has a large impact on the control strategy predictions of models that are more sophisticated than the simple Lagrangian box model on which EKMA is based. A secondary objective was to compare the predictions of the different models selected for the purpose of identifying (1) those factors that must be rationalized to obtain similar results, and (2) those that preclude similar results (e.g., grid dispersion models predict intrinsically different results than trajectory models for cases in which high wind shear is a factor).

One of the four kinetic mechanisms examined in the study of Jeffries et al. (1981)--CBM-II (Whitten et al., 1980)--is already implemented in a photochemical dispersion model that has been validated for a number of urban areas including Los Angeles. The CBM-II has also been implemented in a multicell trajectory model, a reactive plume model, and a sophisticated Lagrangian box model using the OZIPM/EKMA methodology; this methodology was employed by the South Coast Air Quality Management District in its revisions to the 1982 SIP for air pollution control in the Los Angeles area. Thus, an extensive data base for model comparisons exists.

BEGIN LAST LINE OF TEXT
BOTTOM OF IMAGE AREA, OUTSIDE DIMENSION FOR TABLES AND ILLUSTRATIONS
3/8"

PAGE NUMBER
EPA-287 (Cin.)
(4-76)

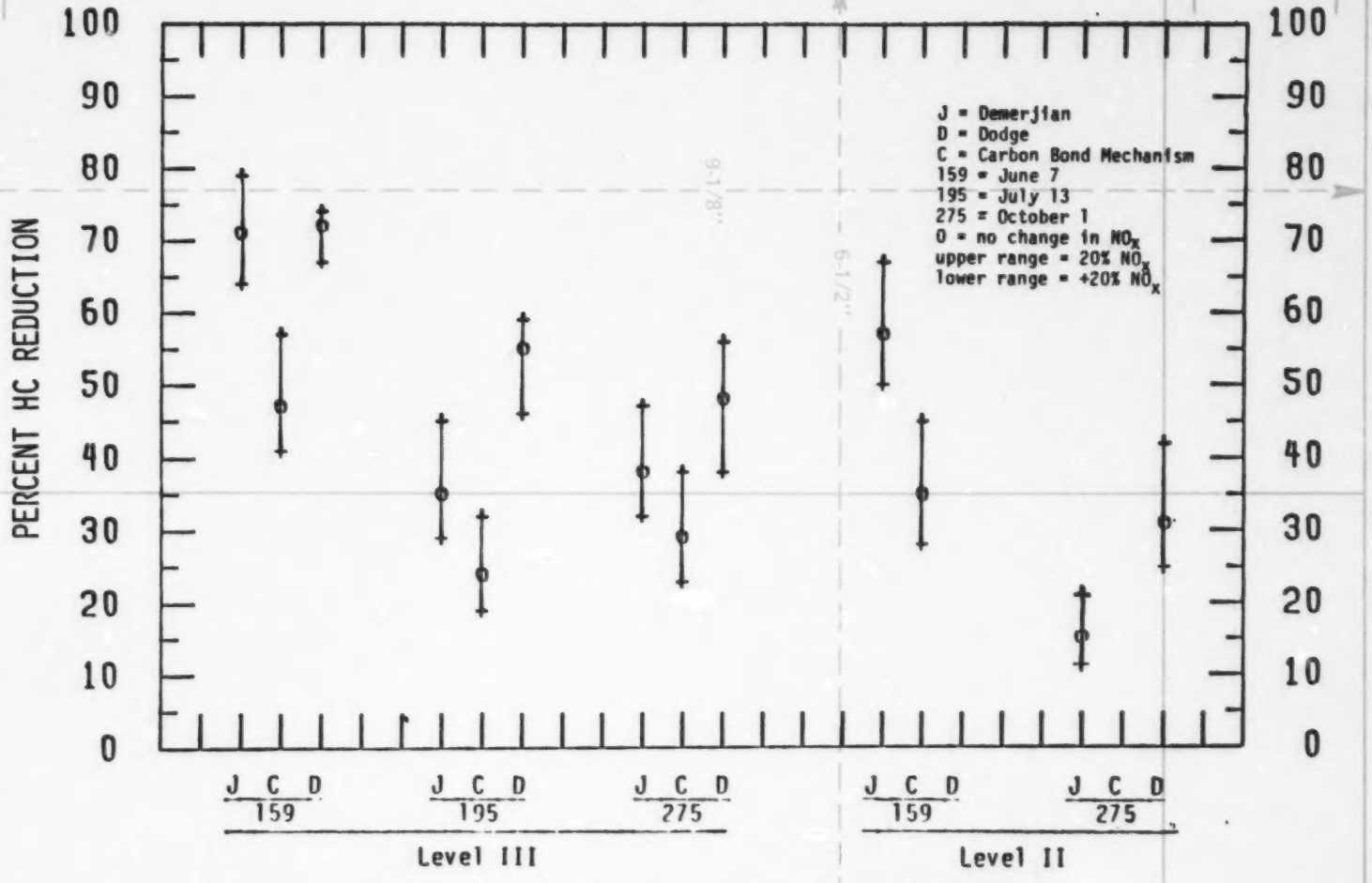

Figure 1. Control predictions for three NO_x control conditions by method/day/mechanism. (Characteristic curve mixing-height profile.)

Source: Jeffries et al. (1981)

BEGIN FIRST LINE OF TEXT HERE
TYPING GUIDE SHEET
CENTER OF PAGE
TOP OF IMAGE AREA
DROPPED HEAD: BEGIN SECTIONS HERE

We eliminated from consideration two of the remaining three mechanisms considered by Jeffries et al. (1981). The Dodge mechanism used in the standard EKMA is a propene/butane surrogate mechanism whose simulation of the behavior of auto exhaust has been been validated with the BOM data. There is currently no clear methodology, however, for extending this mechanism to other source categories, or for accounting for changes in hydrocarbon speciation. Moreover, a number of the reaction rate constants are not in keeping with currently accepted values; revision of these rate constants would necessitate revalidation of the mechanism, a task beyond the scope of this project.

Jeffries et al. (1981) found the CIT mechanism (Falls and Seinfeld, 1978) to be inadequate for simulating the BOM data at higher NO_x levels. Since the publication of their work, the CIT mechanism has been modified in regard to a number of important stoichiometric parameters. As in the case of the Dodge mechanism, however, revalidation of the CIT mechanism was beyond the scope of this effort. Therefore, we selected the Demerjian photochemical box model (DPBM) mechanism for comparison with the CBM-II in the Airshed and trajectory model simulations. The Los Angeles data base was used for this study.

9-1/8"
BEGIN LAST LINE OF TEXT
BOTTOM OF IMAGE AREA, OUTSIDE DIMENSION FOR TABLES AND ILLUSTRATIONS
3/8"

EPA-287 (Cin.)
(4-76)

BEGIN FIRST LINE OF TEXT HERE
TYPING GUIDE SHEET
CENTER OF PAGE
TOP OF IMAGE AREA
DROPPED HEAD; BEGIN SECTIONS HERE

SECTION 2

AIRSHED MODEL CALCULATIONS OBTAINED USING THE DPBM MECHANISM

The Demerjian Photochemical Box Model Mechanism is a lumped species mechanism with four organic classes: olefins, paraffins, aromatics, and aldehydes. In contrast to the Carbon-Bond Mechanism, which treats subcomponents of molecules (reactive structures) as the basic unit of reaction, in the DPBM Mechanism lumping is accomplished at the molecular level; each reactive organic molecule is assumed to belong to one of the four classes. The organic classes in the DPBM have an assumed average carbon number that need not be an integer, whereas the carbon number for each reactive structure in the CBM is invariant and is always an integer.

Implementation of the DPBM Mechanism (shown in Table 1) in the Urban Airshed Model was accomplished using standard procedures for computation of steady-state values for radical species and a finite-difference scheme for computation of transported species. The radical species O, NO_3, OH, HO_2, RO_2, $R1O_2$, RO, $R2O_2$, and R2O were assumed to be in steady state, whereas concentrations of NO, NO_2, O_3, HNO_2, HO_4N, OLE, PAR, ALD, PAN, ARO, and CO were computed using a finite-difference scheme. The subroutine CHEM, used to compute steady-state approximations and chemical reaction rates, is given in Appendix A.

Emission, boundary, and initial-condition inputs to the grid model were easily modified. Molar concentrations of ARO and ALD are the same for both the CBM and the DPBM (ALD is CARB in the CBM). The DPBM species OLE is the sum of OLE and ETH in the CBM. All carbon in the DPBM species over that accounted for by the CBM carbon structures must be subtracted from the PAR species in the CBM. For example, ARO has six carbons, whereas in the DPBM, the carbon number of ARO is 8.1. Thus, 2.1 carbons must be subtracted from the PAR group in the CBM before it can be converted to molecular units for use in the DPBM mechanism. Carbon numbers for the DPBM catagories are taken from Jeffries et al. (1981) (Table 2).

BEGIN LAST LINE OF TEXT
BOTTOM OF IMAGE AREA; OUTSIDE DIMENSION FOR TABLES AND ILLUSTRATIONS
3/8"

PAGE NUMBER
EPA-287 (Cin.) (4-76)

BEGIN FIRST LINE OF TEXT HERE
TYPING GUIDE SHEET
CENTER OF PAGE
TOP OF IMAGE AREA
DROPPED HEAD; BEGIN SECTIONS HERE

TABLE 1. THE DEMERJIAN PHOTOCHEMICAL BOX MODEL MECHANISM

NUM	REACTANTS				PRODUCTS				A FACTOR	STD RATE U
1)			NO2	--HV--> 1.00	NO	+ 1.00	O		1.000E+00	<5.000E-01>1
2)			O	------> 1.00	O3				4.200E+06	<4.200E+06>1
3)	O3	+	NO	------> 1.00	NO2				2.200E+01	<2.200E+01>2
4)	O3	+	NO2	------> 1.00	NO3				5.500E-02	<5.500E-02>2
5)	NO3	+	NO	------> 2.00	NO2				1.100E+04	<1.100E+04>2
6)	NO3	+	NO2	(PZU) ------> 2.00	WHNO3				8.400E-03	<4.000E+01>2
7)			HNO2	--HV--> 1.00	HO	+ 1.00	NO		1.666E-01	<9.330E-02>1
8)	HO	+	CO	------> 1.00	HO2	+ 1.00	CO2		4.400E+02	<4.400E+02>2
9)	HO2	+	NO2	------> 1.00	HNO2				4.300E+00	<4.300E+00>2
10)	HO2	+	NO	------> 1.00	HO	+ 1.00	NO2		1.200E+04	<1.200E+04>2
11)	HO2	+	NO2	------> 1.00	HO4N				2.340E+03	<2.340E+03>2
12)			HO4N	------> 1.00	HO2	+ 1.00	NO2		9.000E+00	<9.000E+00>1
13)	HO	+	HNO2	------> 1.00	NO2				9.600E+03	<9.600E+03>2
14)	HO	+	NO2	------> 1.00	HNO3				1.500E+04	<1.500E+04>2
15)	HO	+	NO	------> 1.00	H2O2				1.200E+04	<1.200E+04>2
16)	HO2	+	O3	------> 1.00	HO				4.000E+00	<4.000E+00>2
17)	HO	+	O3	------> 1.00	HO2				8.700E+01	<8.700E+01>2
18)	HO2	+	HO2	------> 0.50	H2O2				1.000E+04	<1.000E+04>2
19)	OLE	+	O	------> 1.00	RO2	+ 1.00	ALD	+ 1.00 HO2	9.100E+03	<5.100E+03>2
20)	OLE	+	O3	--- --> 1.00	RO2	+ 1.00	ALD	+ 1.00 HO2	1.700E-02	<1.700E-02>2
21)	OLE	+	HO	------> 1.00	RO2	+ 1.00	ALD		3.700E+04	<3.700E+04>2
22)	PAR	+	HO	------> 1.00	RO2				5.000E+03	<5.000E+03>2
23)			ALD	--UV--> 0.50	RO2	+ 1.50	HO2	+ 1.00 CO	1.000E+00	<1.900E-03>1
24)	ALD	+	HO	------> 0.50	R1O2	+ 0.50	HO2		2.200E+04	<2.200E+04>2
25)	RO2	+	NO	------> 1.00	RO	+ 1.00	NO2		2.000E+03	<2.000E+03>2
26)			RO	------> 1.00	ALD	+ 1.00	HO2		9.240E+02	<9.240E+02>1
27)	R1O2	+	NO2	------> 1.00	PAN				2.100E+03	<2.100E+03>2
28)	HO	+	NO2	------> 1.00	RNO3				1.200E+02	<1.200E+02>2
29)	HO2	+	O3	------> 1.00	HO				2.000E+00	<2.000E+00>2
30)	R1O2	+	NO	------> 1.00	RO2	+ 1.00	NO2		3.800E+03	<3.800E+03>2
31)			PAN	------> 1.00	R1O2	+ 1.00	NO2		1.100E-01	<1.100E-01>1
32)	ARO	+	HO	------> 1.00	R2O2	+ 2.00	ALD	+ 1.00 CO	2.000E+04	<2.000E+04>2
33)	R2O2	+	NO	------> 1.00	R4O	+ 1.00	NO2		2.000E+03	<2.000E+03>2
34)			R2O	------> 1.00	ALD	+ 1.00	HO2	+ 2.00 CO	2.100E+03	<2.100E+03>1
35)	R2O2	+	O3	------> 1.00	R2O				2.000E+00	<2.000E+00>2
36)	R1O2	+	O3	------> 1.00	RO2				2.000E+00	<2.000E+00>2
37)			NR	------> 1.00	NR				1.000E-06	<1.000E-06>1

Reproduced from best available copy.

BEGIN LAST LINE OF TEXT
3/8"
BOTTOM OF IMAGE AREA OUTSIDE DIMENSION FOR TABLES AND ILLUSTRATIONS

EPA-287 (Cin.)
(4-76)

BEGIN FIRST LINE OF TEXT HERE
TYPING GUIDE SHEET
CENTER OF PAGE
TOP OF IMAGE AREA
DROPPED HEAD; BEGIN SECTIONS HERE

TABLE 2. CARBON NUMBERS FOR SPECIES IN CBM AND DPBM

	Species	Carbon No.
CBM II		
	ETH	2
	OLE	2
	CARB	1
	PAR	1
	ARO	6
DPBM		
	OLE	3
	ARO	8.1
	ALD	1
	PAR	6

Unambiguous species such as NO, NO_2, O_3, and PAN were directly converted. Emission, boundary and initial concentrations of trace species not common to both mechanisms (such as GLY for CBM and HONO and HNO_4 for DPBM) were assumed to be low enough to be neglected in the translation process.

The final requirement for implementing the DPBM mechanism in the Airshed Model was the selection of a lumped aldehyde photolysis rate. For our simulations, we chose a rate for Reaction 23 (Table 1) of 1.9×10^{-3} times the rate of NO_2 photolysis (k_1). This is essentially the same rate ratio that was used in the DPBM mechanism validation simulations of auto exhaust experiments. Furthermore, it is within 5 percent of the lumped carbonyl photolysis rate used in the CBM atmospheric simulations.

RESULTS OF THE BASE-CASE AIRSHED MODEL SIMULATION USING THE DPBM MECHANISM

The Airshed Model simulation using the DPBM mechanism was initialized at 0500 for the 27 June base case described in Killus et al. (1981). As illustrated in Figure 2, the simulation provides a good fit to the data. The DPBM mechanism generally predicts slightly higher ozone values than the CBM-II, with the greatest discrepancy occurring for intermediate ozone values (15-30 pphm).

Because the Airshed Model simulations using the CBM-II slightly overpredict the station averaged ozone for the 27 June base case, the DPBM mechanism overpredicts average ozone values by a slightly greater margin. However, the difference is essentially trivial; factors other than the choice

BEGIN LAST LINE OF TEXT
BOTTOM OF IMAGE AREA; OUTSIDE DIMENSION FOR TABLES AND ILLUSTRATIONS
3/8"

PAGE NUMBER
EPA-287 (Cin.) (4-78)

BEGIN FIRST LINE OF TEXT HERE
TYPING GUIDE SHEET
CENTER OF PAGE
TOP OF IMAGE AREA
DROPPED HEAD; BEGIN SECTIONS HERE

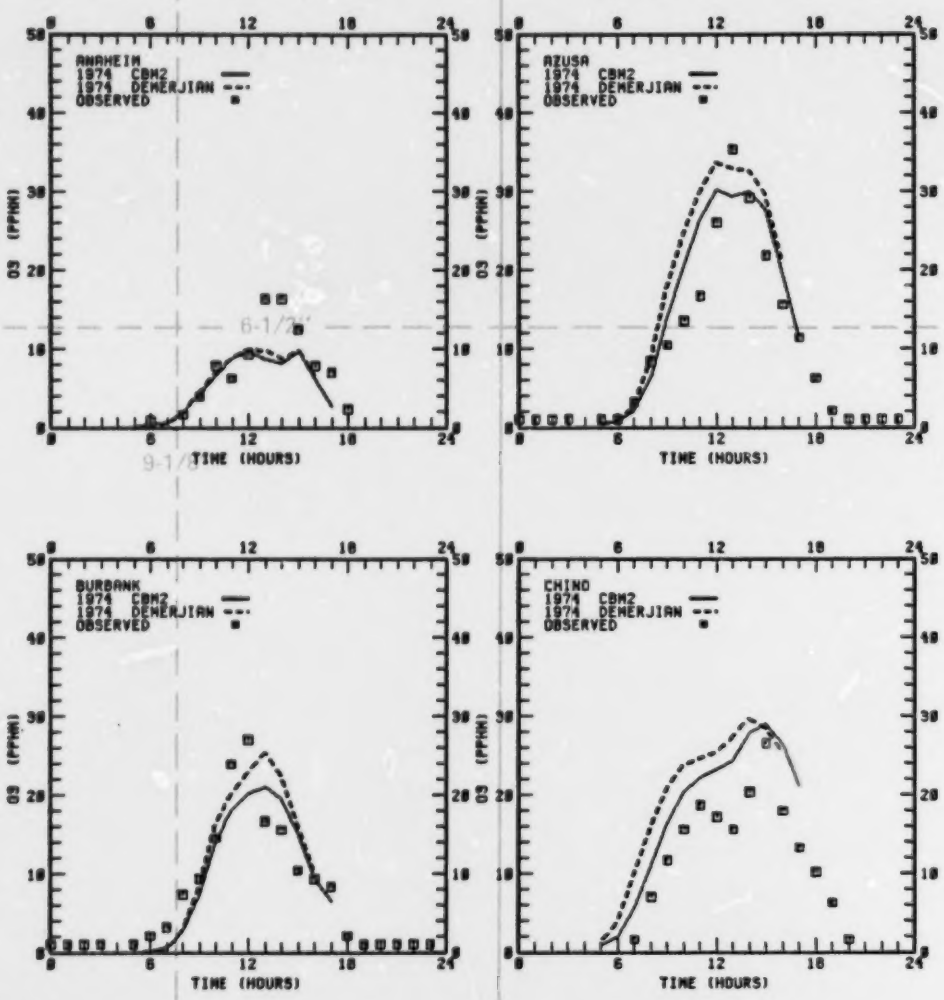

Figure 2. Comparison of O_3 results for Los Angeles, 27 June 1974, (Airshed base case) for the DPBM mechanism and CBM-II.

BEGIN LAST LINE OF TEXT
BOTTOM OF IMAGE AREA; OUTSIDE DIMENSION FOR TABLES AND ILLUSTRATIONS
3/8"

EPA-287 (Cin.)
(4-76)

BEGIN FIRST LINE OF TEXT HERE
TYPING GUIDE SHEET
CENTER OF PAGE
TOP OF IMAGE AREA
DROPPED HEAD; BEGIN SECTIONS HERE
6-1/2"

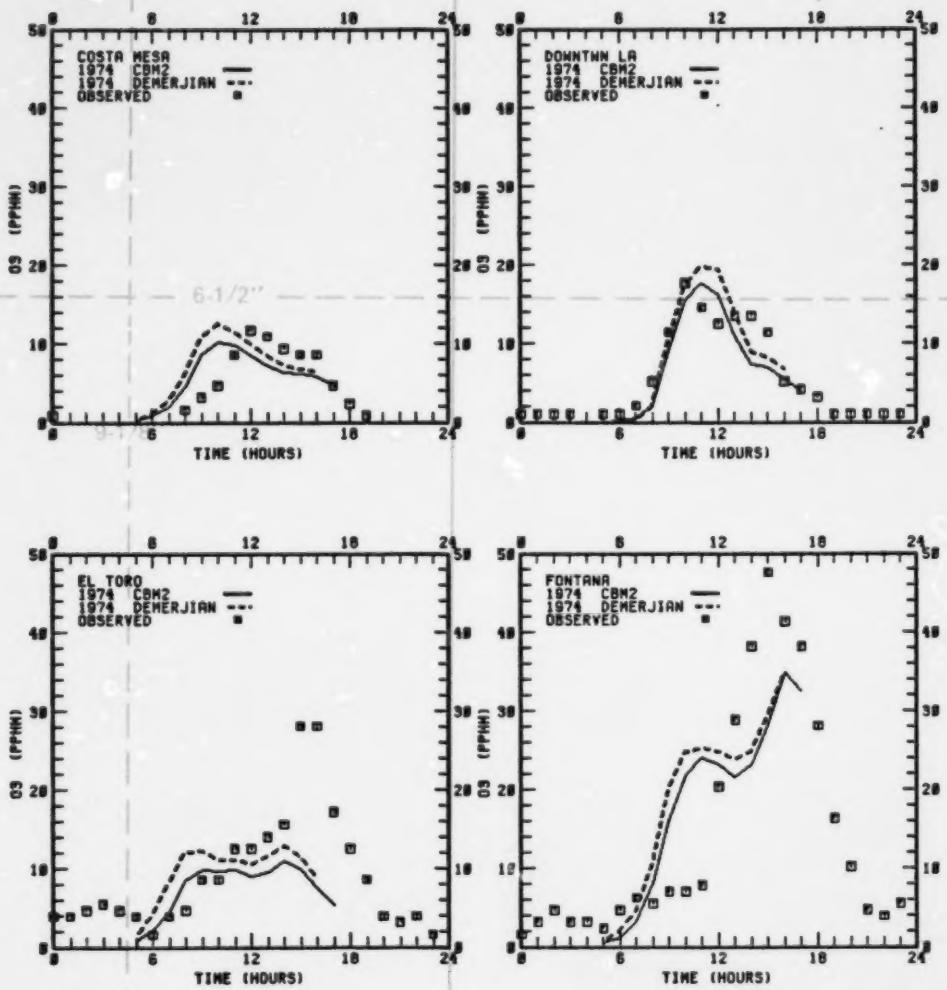

Figure 2. (continued).

BEGIN LAST LINE OF TEXT
BOTTOM OF IMAGE AREA OUTSIDE DIMENSION FOR TABLES AND ILLUSTRATIONS
3/8"

EPA-287 (Cin.)
(4-76)

BEGIN FIRST LINE OF TEXT HERE
TYPING GUIDE SHEET
CENTER OF PAGE
TOP OF IMAGE AREA
DROPPED HEAD; BEGIN SECTIONS HERE
6-1/2"

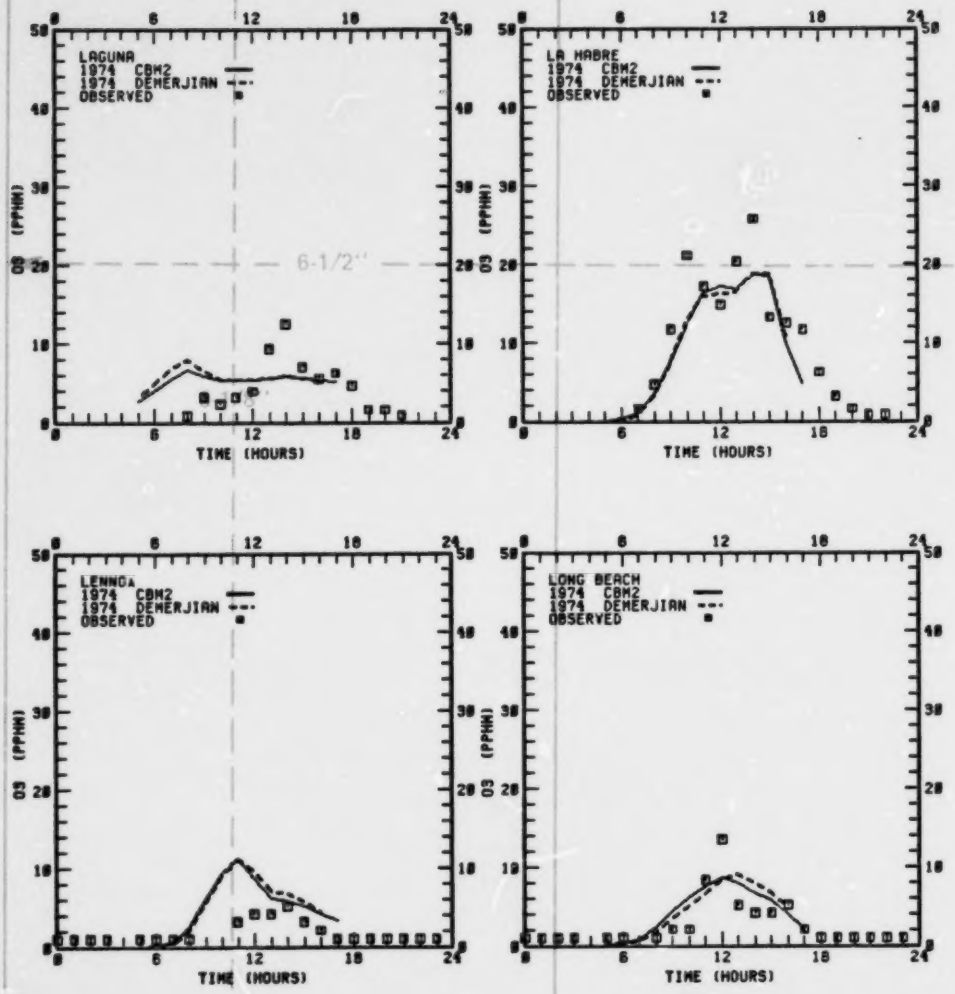

Figure 2. (continued).

BEGIN LAST LINE OF TEXT
3/8"
BOTTOM OF IMAGE AREA, OUTSIDE DIMENSION FOR TABLES AND ILLUSTRATIONS

EPA-287 (Cin.)
(4-76)

BEGIN FIRST LINE OF TEXT HERE
TYPING GUIDE SHEET
CENTER OF PAGE
TOP OF IMAGE AREA
DROPPED HEAD; BEGIN SECTION HERE

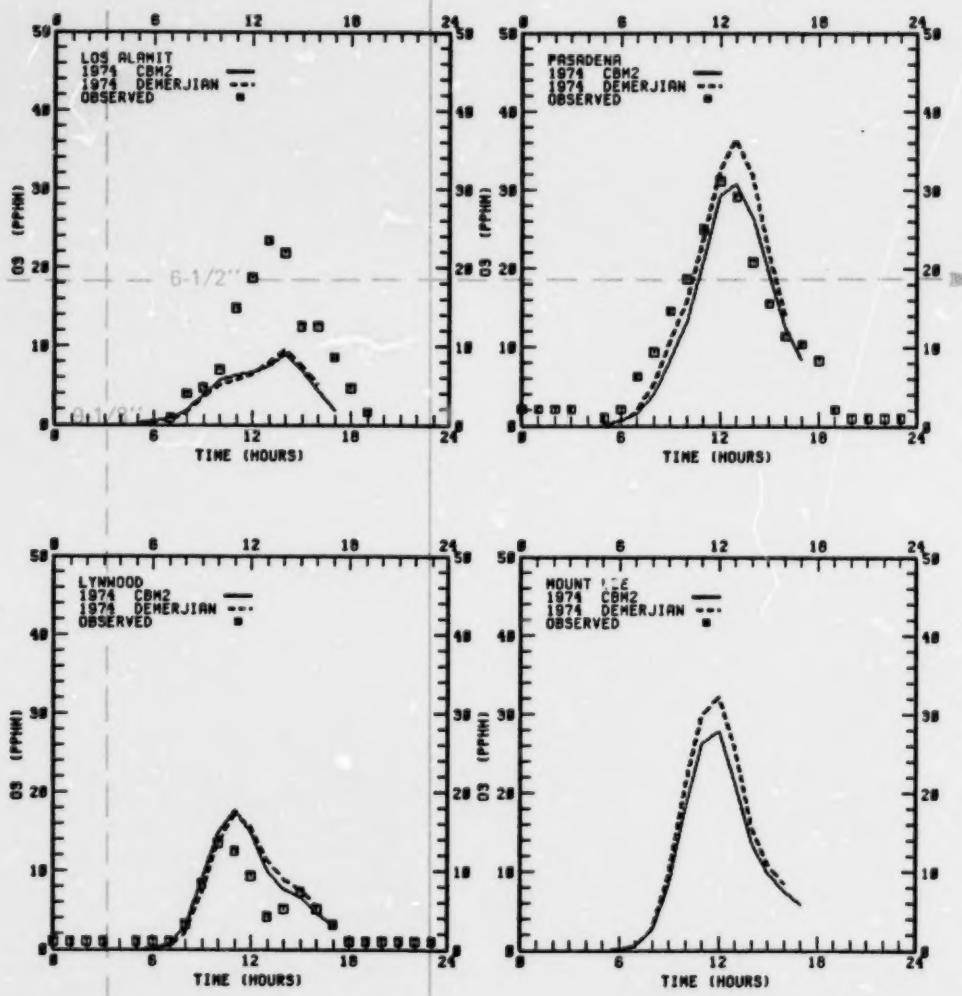

Figure 2. (continued).

BEGIN LAST LINE OF TEXT
BOTTOM OF IMAGE AREA OUTSIDE DIMENSION FOR TABLES AND ILLUSTRATIONS
3/8"

EPA-287 (Cin.)
(4-76)

BEGIN FIRST LINE OF TEXT HERE
TYPING GUIDE SHEET
CENTER OF PAGE
TOP OF IMAGE AREA
DROPPED HEAD; BEGIN SECTIONS HERE
6-1/2"
9-1/8"

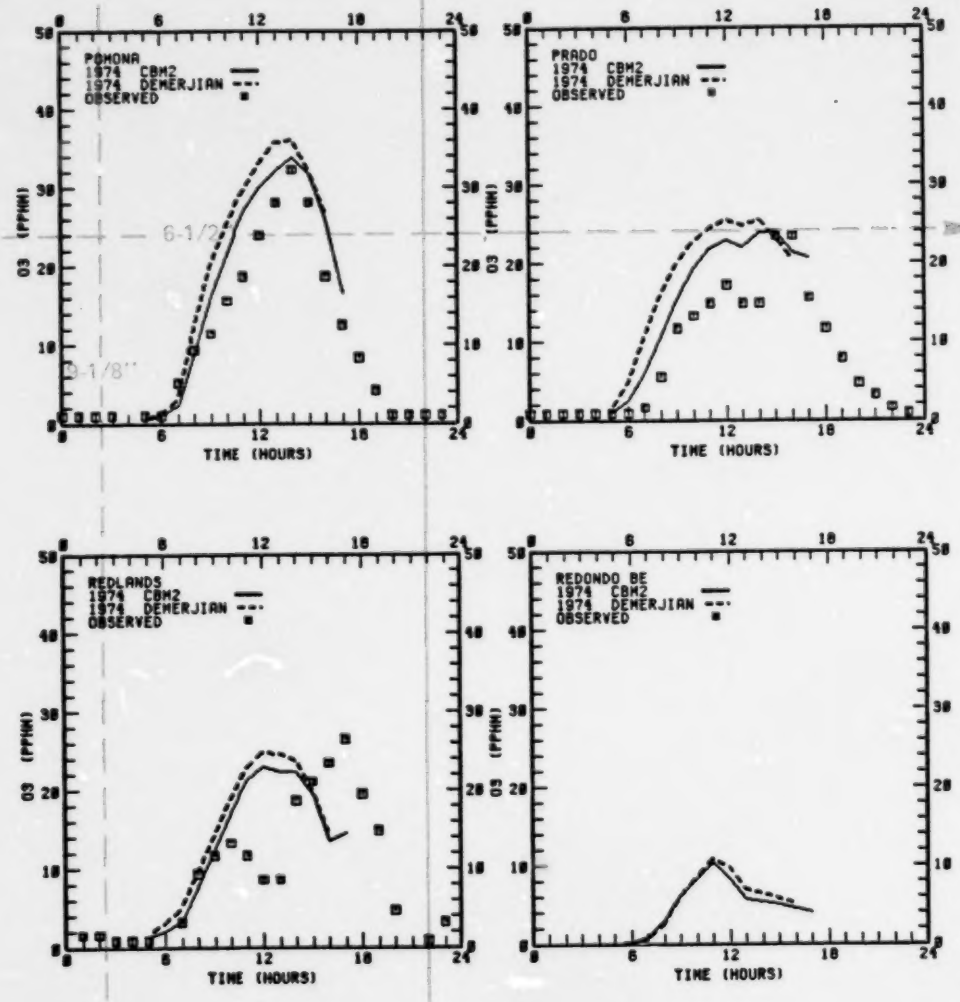

Figure 2. (continued).

BEGIN LAST LINE OF TEXT
BOTTOM OF IMAGE AREA; OUTSIDE DIMENSION FOR TABLES AND ILLUSTRATIONS
3/8"

EPA-287 (Cin.)
(4-76)

BEGIN FIRST LINE OF TEXT HERE
TYPING GUIDE SHEET
CENTER OF PAGE
TOP OF IMAGE AREA
DROPPED HEAD; BEGIN SECTIONS HERE
6-1/2"
9-1/8"

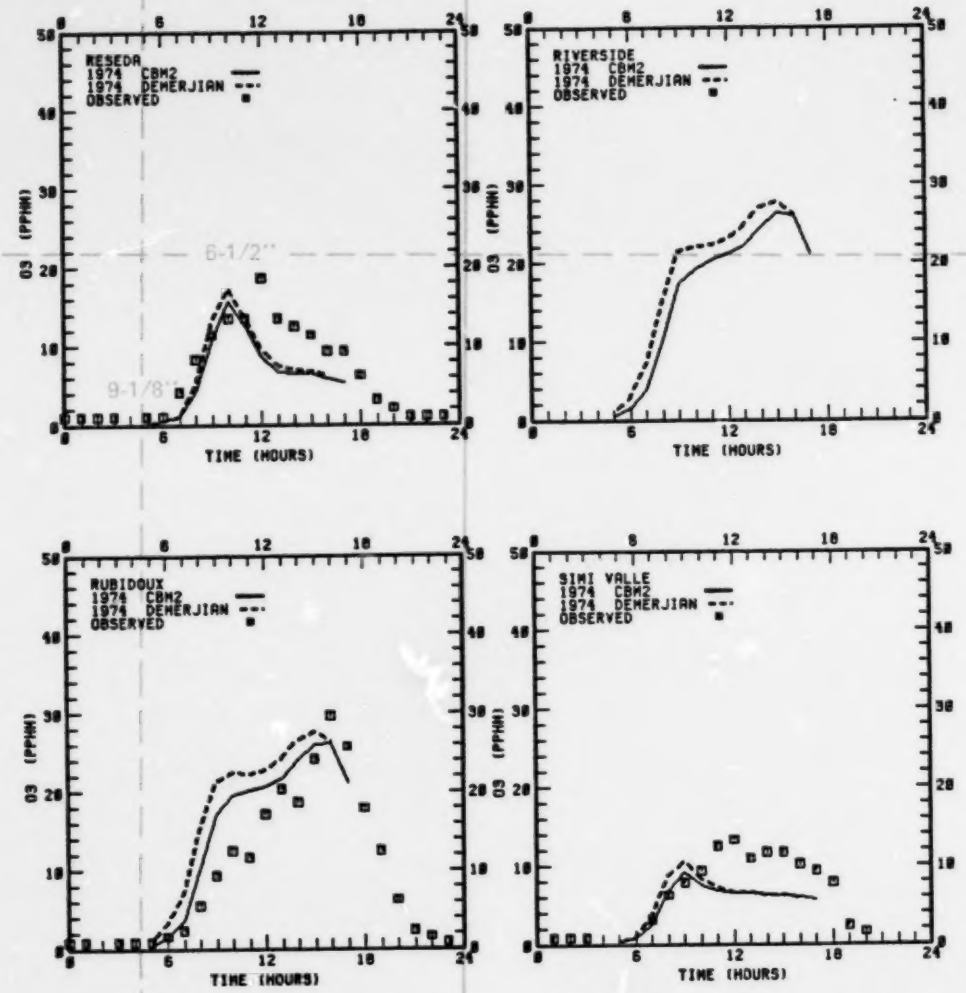

Figure 2. (continued).

BEGIN LAST LINE OF TEXT
BOTTOM OF IMAGE AREA; OUTSIDE DIMENSION FOR TABLES AND ILLUSTRATIONS
3/8"

EPA-287 (Cin.)
(4-76)

BEGIN FIRST LINE OF TEXT HERE
TYPING GUIDE SHEET
CENTER OF PAGE
TOP OF IMAGE AREA
DROPPED HEAD; BEGIN SECTIONS HERE
6-1/2"
9-1/8"

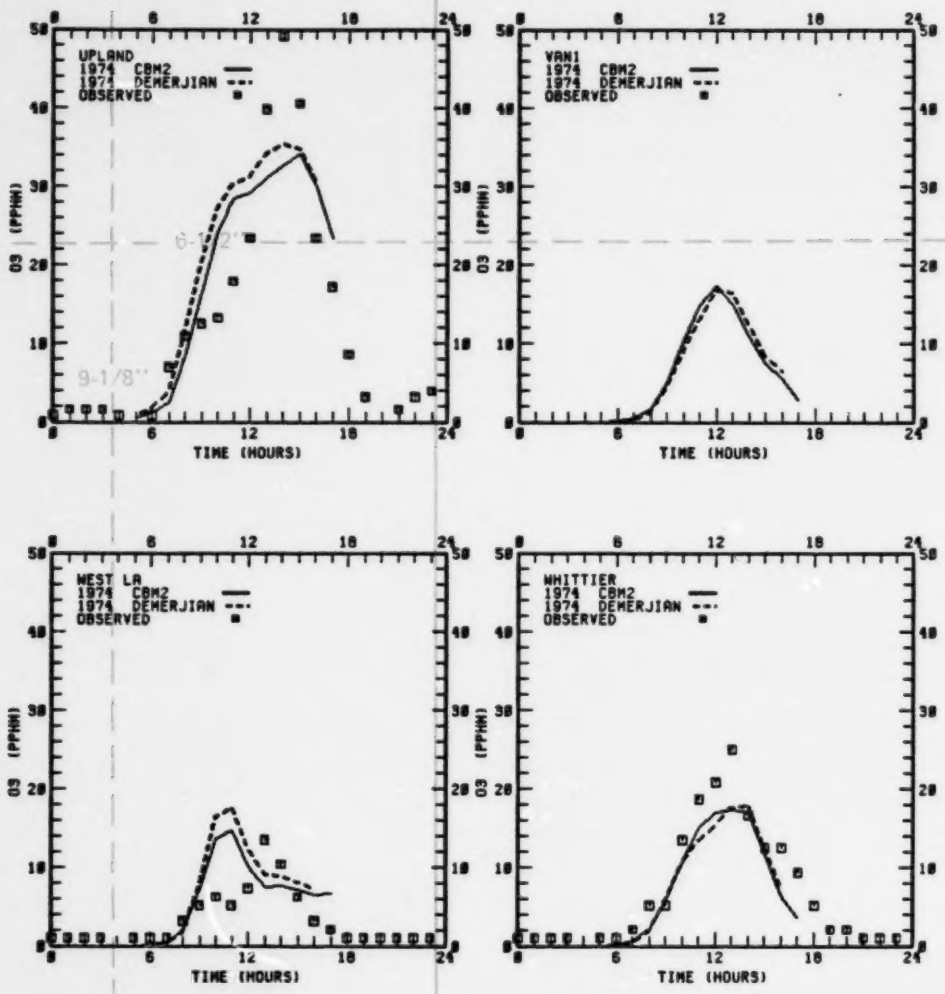

Figure 2. (concluded).

BEGIN LAST LINE OF TEXT
BOTTOM OF IMAGE AREA; OUTSIDE DIMENSION FOR TABLES AND ILLUSTRATIONS
3/8"

EPA-287 (Cin.)
(4-76)

BEGIN FIRST LINE OF TEXT HERE
TYPING GUIDE SHEET
CENTER OF PAGE
TOP OF IMAGE AREA

of kinetic mechanism, such as wind fields, mixing depths, etc., have a greater effect on model calculations for the 27 June base case.

DROPPED HEAD; BEGIN SECTIONS HERE

When the 1987 emission inventory is used (Figure 3), the DPBM mechanism predicts lower ozone concentrations than the CBM-II at most of the stations in the modeling domain. This finding apparently contradicts the results of Jeffries et al. (1981), who found that predictions obtained with the CBM-II showed a greater response to hydrocarbon control than predictions obtained with the DPBM mechanism. The Airshed Model results using the DPBM mechanism predict from 10 to 35 percent greater ozone reduction than when the CBM-II was used for the 1987 control scenario (Table 3).

We believe that this result is due to the shift in hydrocarbon speciation that occurs in the 1987 inventory relative to 1974. The effect of the control measures is to reduce the carbon mole fraction (in DPBM units) of olefins from about 0.2 in 1974 to 0.15 in 1987 (see Table 4). The DPBM mechanism is quite sensitive to the olefin fraction (see Appendix B); thus a reduction in the olefin fraction could be expected to have a greater effect on DPBM predictions than on CBM predictions. We address this point in greater detail in the next section.

9-1/8"

TABLE 3. AIRSHED RESULTS FOR 1974 AND 1987 SCENARIOS

Station (time)	CBMII (pphm O_3)		% Change	DPBM (pphm O_3)		% Change
	1974	1987		1974	1987	
Fontana (1600-1700)	34.9	24.9	-29	34.8	22.6	-35
Cell (25, 14) highest ozone** (1600-1700)	39	29	-26	40	24	-40
Upland (1500-1600)	23.1	23.1	-32	34.9	19.8	-43
Downtown Los Angeles (1100-1200)	17.6	9.72 (1200-1300)*	-45	19.8	9.6 (1200-1300)*	-51
Pasadena (1300-1400)	30.8	15.7	-49	36.4	14.4	-60

* Control Strategy produced a delay in the ozone peak of one hour.
** Cell concentrations reported in pphm; output concentrations at monitors are in ppb.

BEGIN LAST LINE OF TEXT
BOTTOM OF IMAGE AREA OUTSIDE DIMENSION FOR TABLES AND ILLUSTRATIONS
3/8"

PAGE NUMBER
EPA-287 (Cin.) (4-76)

BEGIN FIRST LINE OF TEXT HERE
TYPING GUIDE SHEET
CENTER OF PAGE
TOP OF IMAGE AREA
DROPPED HEAD; BEGIN SECTIONS HERE
6-1/2"
9-1/8"

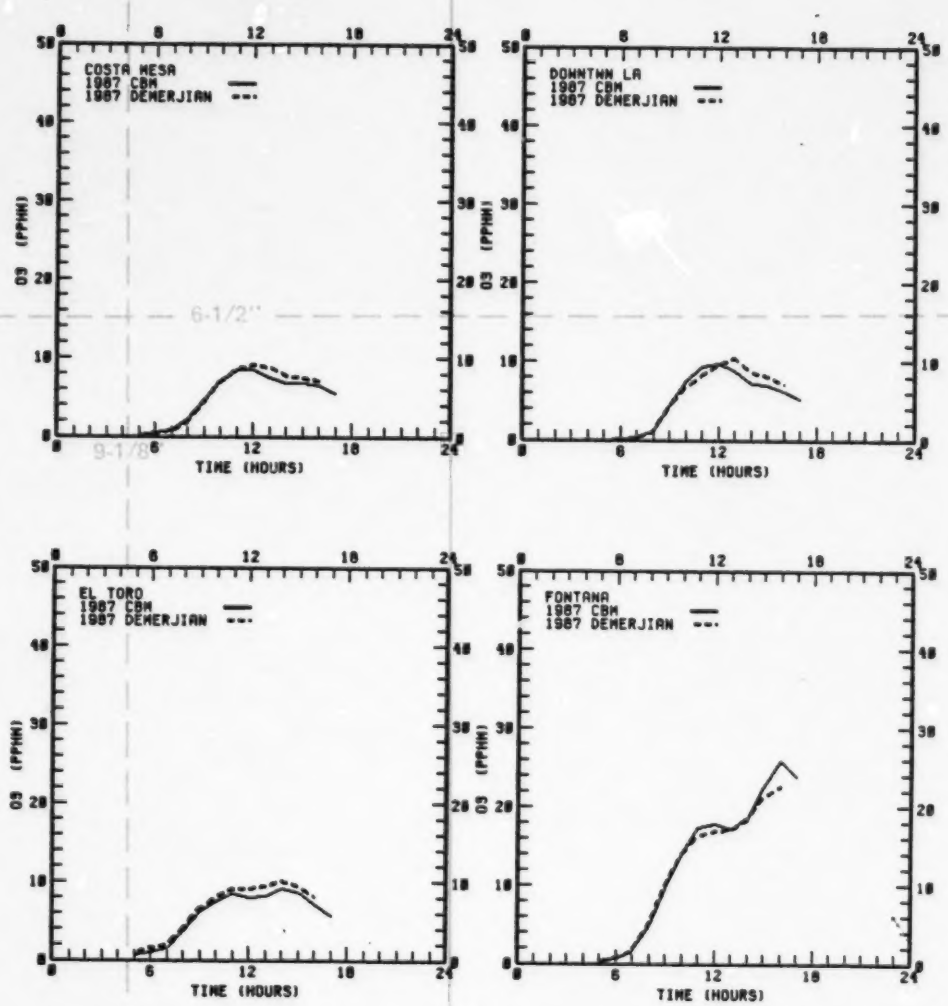

Figure 3. Comparison of O_3 results for Los Angeles, 27 June 1987, for the DPBM mechanism and the CBM-II.

BEGIN LAST LINE OF TEXT
BOTTOM OF IMAGE AREA; OUTSIDE DIMENSION FOR TABLES AND ILLUSTRATIONS
3/8"

EPA-287 (Cin.)
(4-76)

BEGIN FIRST LINE OF TEXT HERE
TYPING GUIDE SHEET
CENTER OF PAGE
TOP OF IMAGE AREA
DROPPED HEAD; BEGIN SECTIONS HERE
6-1/2"
9-1/8"

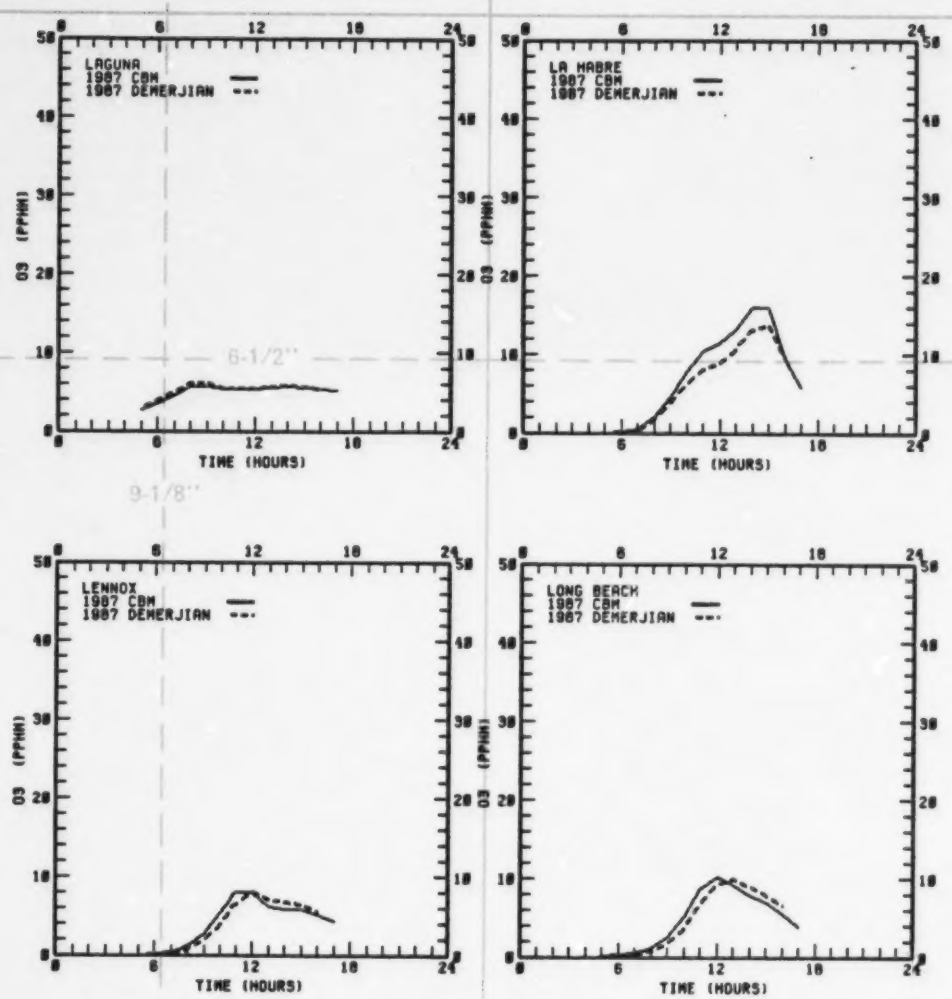

Figure 3. (continued).

BEGIN LAST LINE OF TEXT
BOTTOM OF IMAGE AREA; OUTSIDE DIMENSION FOR TABLES AND ILLUSTRATIONS
3/8"

EPA-287 (Cin.)
(4-76)

BEGIN FIRST LINE OF TEXT HERE
TYPING GUIDE SHEET
CENTER OF PAGE
TOP OF IMAGE AREA
DROPPED HEAD; BEGIN SECTIONS HERE
6-1/2"
9-1/8"

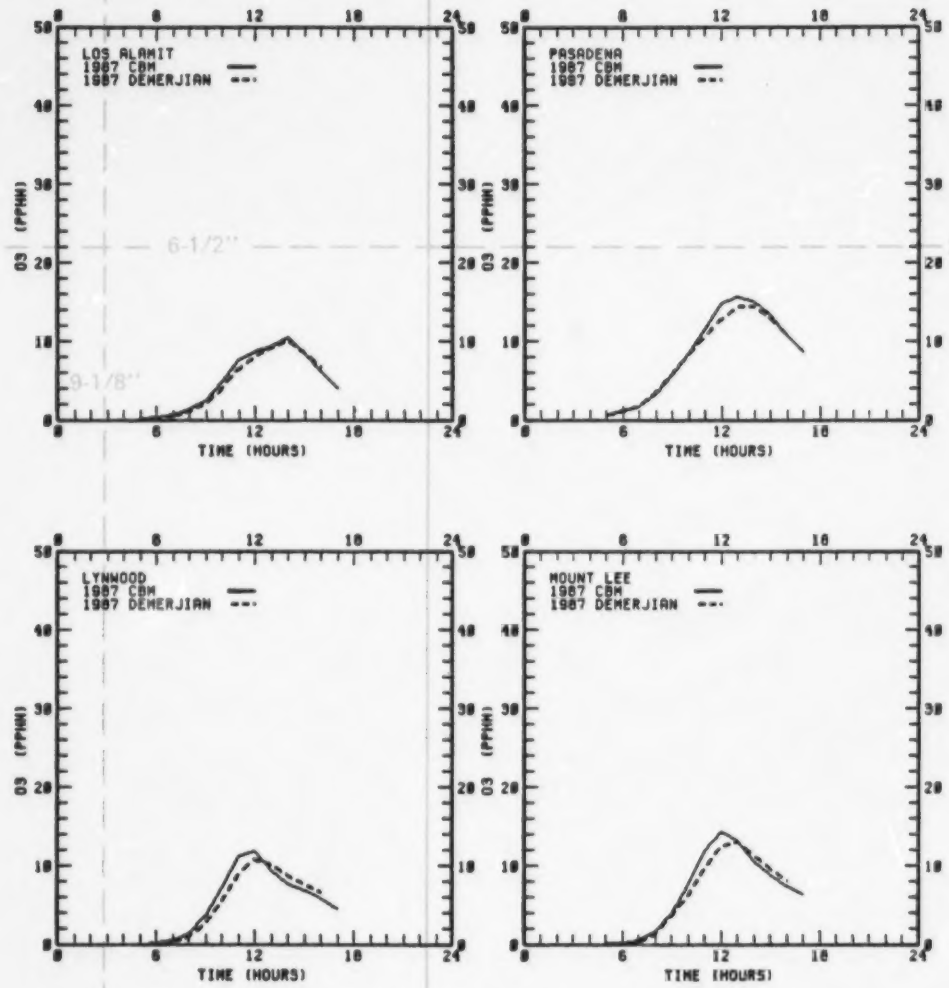

Figure 3. (continued).

BEGIN LAST LINE OF TEXT
3/8"
BOTTOM OF IMAGE AREA OUTSIDE DIMENSION FOR TABLES AND ILLUSTRATIONS

EPA-287 (Cin.)
(4-76)

BEGIN FIRST LINE OF TEXT HERE
TYPING GUIDE SHEET
CENTER OF PAGE
TOP OF IMAGE AREA
DROPPED HEAD; BEGIN SECTIONS HERE
6-1/2"
9-1/8"

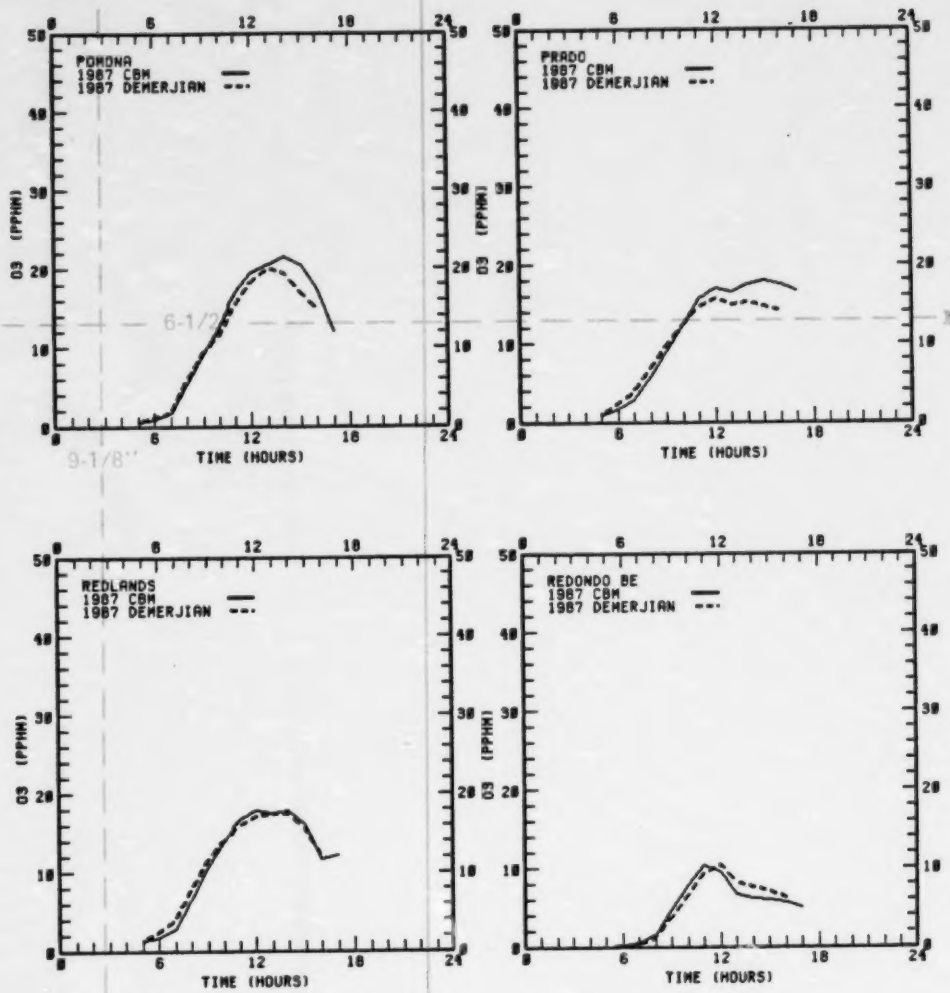

Figure 3. (continued).

BEGIN LAST LINE OF TEXT
3/8"
BOTTOM OF IMAGE AREA; OUTSIDE DIMENSION FOR TABLES AND ILLUSTRATIONS

EPA-287 (Cin.)
(4-78)

BEGIN FIRST LINE OF TEXT HERE
TYPING GUIDE SHEET
CENTER OF PAGE
TOP OF IMAGE AREA
DROPPED HEAD; BEGIN SECTIONS HERE
1/8"
5-1/2"

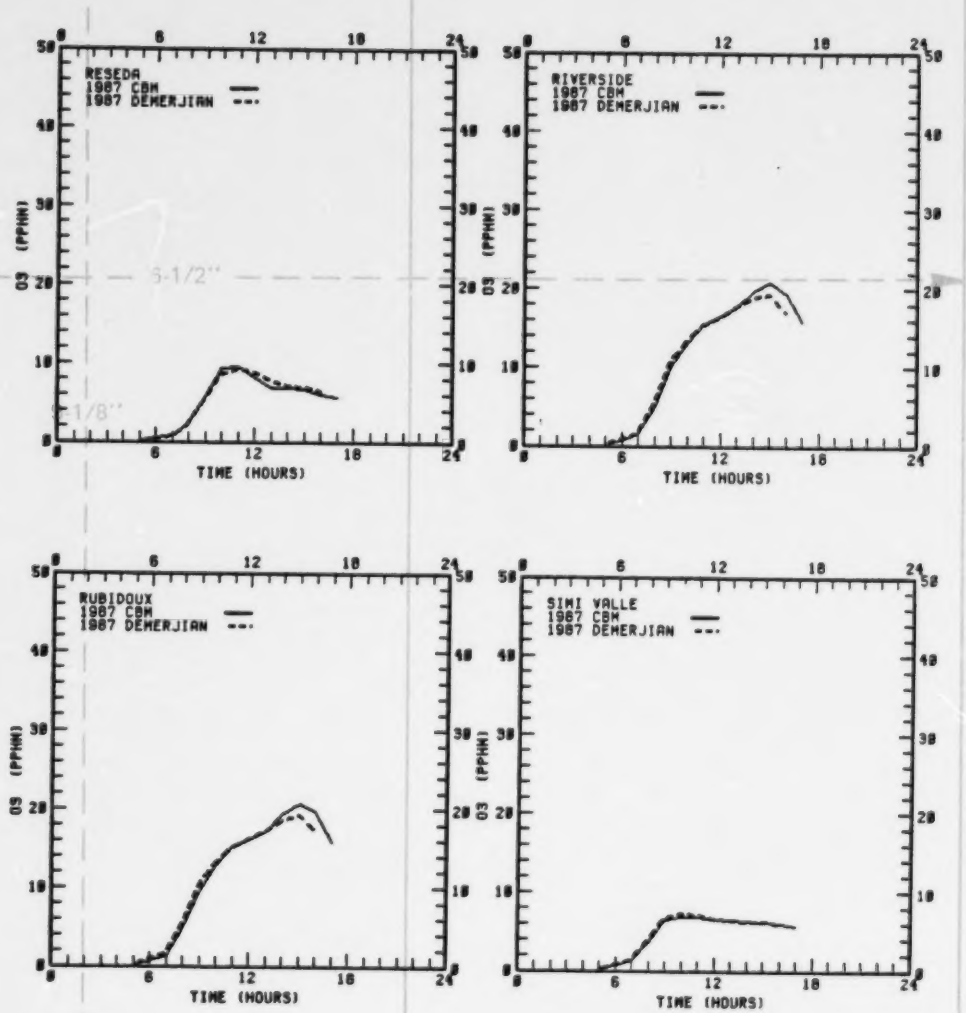

Figure 3. (continued).

BEGIN LAST LINE OF TEXT
BOTTOM OF IMAGE AREA; OUTSIDE DIMENSION FOR TABLES AND ILLUSTRATIONS
3/8"

EPA-287 (Cin.)
(4-76)

BEGIN FIRST LINE OF TEXT HERE
TYPING GUIDE SHEET
CENTER OF PAGE
TOP OF IMAGE AREA
DROPPED HEAD; BEGIN SECTIONS HERE
6-1/2"
9-1/8"

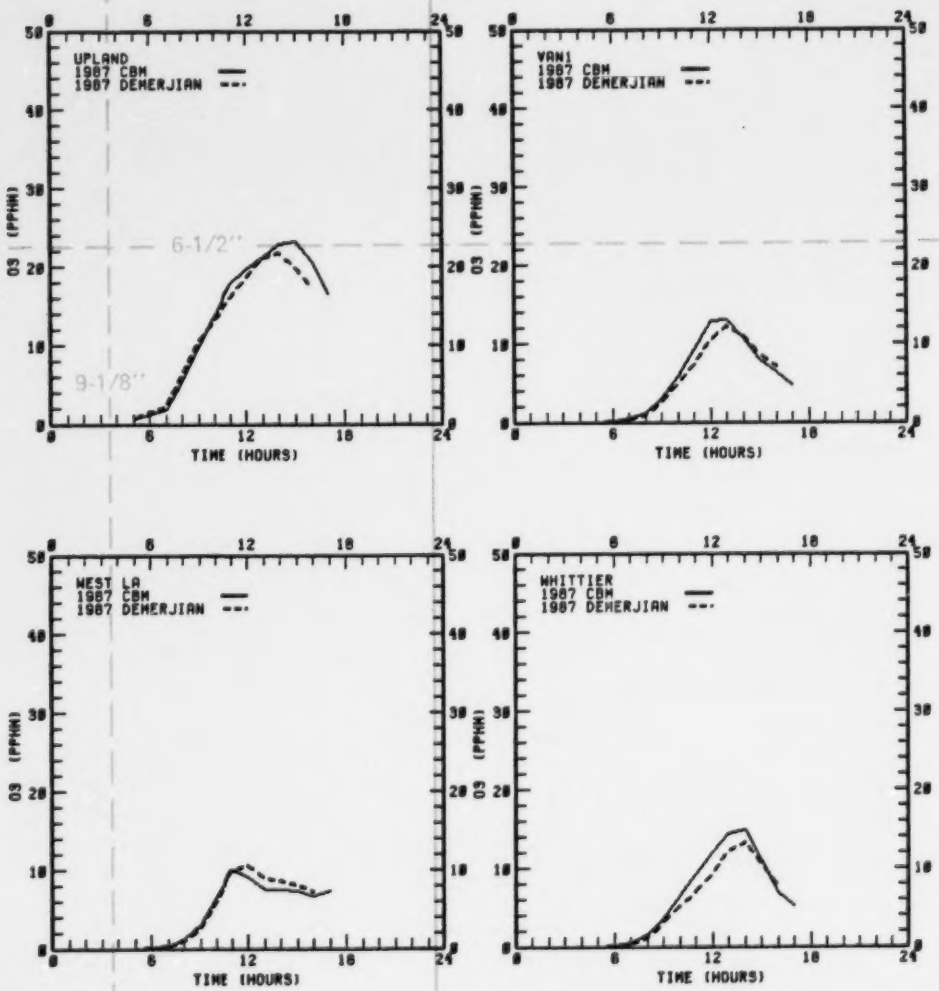

Figure 3. (continued).

BEGIN LAST LINE OF TEXT
BOTTOM OF IMAGE AREA OUTSIDE DIMENSION FOR TABLES AND ILLUSTRATIONS
3/8"

EPA-287 (Cin.)
(4-76)

BEGIN FIRST LINE OF TEXT HERE
TYPING GUIDE SHEET
CENTER OF PAGE
TOP OF IMAGE AREA
DROPPED HEAD; BEGIN SECTIONS HERE
6-1/2"
9-1/8"

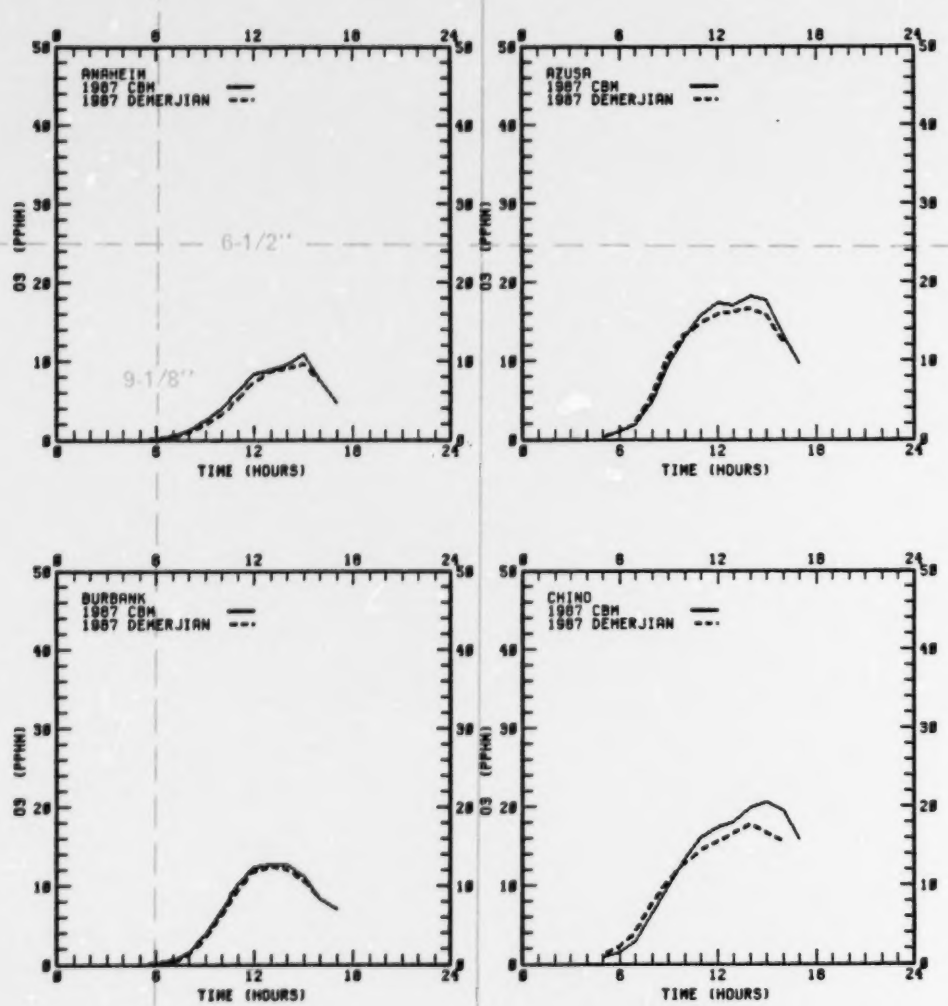

Figure 3. (concluded).

BEGIN LAST LINE OF TEXT
BOTTOM OF IMAGE AREA, OUTSIDE DIMENSION FOR TABLES AND ILLUSTRATIONS
3/8"

PAGE NUMBER
EPA-287 (Cin.)
(4-76)

BEGIN FIRST LINE OF TEXT HERE
TYPING GUIDE SHEET
CENTER OF PAGE
TOP OF IMAGE AREA
DROPPED HEAD; BEGIN SECTIONS HERE
6-1/2"
9-1/8"

TABLE 4. EMISSION INVENTORY INFORMATION

(a) 1974 Emission Inventory
(kilograms/day)

Type of Source	Reactive Organic Compounds (ROG)*	Nitrogen Oxides†
Elevated point sources	7,240	305,540
Nonmotor vehicle area sources	1,007,650	332,640
Motor vehicles	803,980	653,020
All sources	1,818,870	1,291,200

(b) 1987 Baseline Inventory
(kilograms/day)

Type of Source	Reactive Organic Compounds (ROG)*	Nitrogen Oxides†
Elevated point sources	5,860	205,050
Nonmotor vehicle area sources	786,960	321,140
Motor vehicles	215,620	321,230
All sources	1,008,440	847,420

* ROG emissions expressed as methane.
† NO_x emissions expressed as NO_2.

BEGIN LAST LINE OF TEXT
BOTTOM OF IMAGE AREA, OUTSIDE DIMENSION FOR TABLES AND ILLUSTRATIONS
3/8"

EPA-287 (Cin.)
(4-76)

BEGIN FIRST LINE OF TEXT HERE
TYPING GUIDE SHEET
CENTER OF PAGE
TOP OF IMAGE AREA

Continued

DROPPED HEAD; BEGIN SECTIONS HERE

TABLE 4 (Concluded)

(c) Hydrocarbon Splits Used in OZIPM Runs
(obtained from 1974 and 1987 Los Angeles Emissions Inventories)*

DPBM	OLE	PAR	ARO	ALD
1974	0.204	0.506	0.22	0.07
1987	0.153	0.627	0.178	0.042
Carbon number	3.0	6.0	8.1	1.0

6-1/2"

CBM	OLE	PAR	ARO	CARB	ETH
1974	0.055	0.63	0.163	0.07	0.081
1987	0.049	0.728	0.128	0.042	0.053
Carbon number	2	1	6	1	2

9 1/8"

* Atmospheric concentrations are obtained by dividing the carbon fraction by the carbon number. Thus, for 1 ppmC of emissions, [ARO] = 0.22/8.1 = 0.0272 in DPBM; [ARO] = 0.163/6 = 0.0272 in CBM; [OLE] in DPBM = [OLE + ETH] in CBM III. Note that [PAR] does not match in the two mechanisms since $[PAR]_{CBM}$ contains alkyl carbon from molecules that are included in other categories in the DPBM.

BEGIN LAST LINE OF TEXT
BOTTOM OF IMAGE AREA; OUTSIDE DIMENSION FOR TABLES AND ILLUSTRATIONS
3/8"

EPA-287 (Cin.)
(4-76)

BEGIN FIRST LINE OF TEXT HERE
TYPING GUIDE SHEET
CENTER OF PAGE
TOP OF IMAGE AREA
DROPPED HEAD; BEGIN SECTIONS HERE

SECTION 3

COMPARISONS OF THE RESULTS OF SIMPLE AND COMPLEX TRAJECTORY MODELS WITH AIRSHED MODEL RESULTS

To compare the results of the complete grid-based photochemical dispersion model (the Urban Airshed Model) with those of the OZIPM/EKMA model, we employed an intermediate model referred to as the Airshed-Compatible Trajectory Model (ACTM). Development of the ACTM is described in Reynolds et al. (1979).

COMPARISON OF THE ACTM AND AIRSHED MODELS

The ACTM is a trajectory model with chemistry and vertical transport algorithms identical to those contained in the Urban Airshed Model and that uses the same gridded emission inventories and meteorological files. The trajectory is calculated using the first-level wind fields input to the Airshed Model. The ACTM also documents the emissions along a specific trajectory; therefore, it can be used to prepare trajectory-specific emission inputs for other trajectory models such as the EKMA/OZIPM model.

The ACTM calculations were compared to Airshed Model calculations at specific points along the trajectory using interpolation from the four adjacent grid points. The interpolation routine is found in the DISPLAY program, which is also used to compute concentrations at monitoring sites. The trajectory path followed by the ACTM (Figure 4) began at 0500 on 27 June 1974 at a point about seven km southeast of Lennox. The simulated air parcel reached the Fontana area at 1700 hours, near the time of the instantaneous peak ozone value predicted by the Airshed Model for that site. The predicted hourly averaged ozone peak occurred somewhat earlier.

Comparisons of predicted O_3 concentrations for the Airshed Model and the ACTM are very similar along most of the trajectory for both the CBM and DPBM simulations (Figures 5 and 6). The major discrepancy occurs at 1400 hours, when the Airshed model prediction at the trajectory point is markedly lower than the ACTM prediction. However, at this point, the trajectory passes through a region of high wind shear at the base of the

BEGIN LAST LINE OF TEXT
BOTTOM OF IMAGE AREA; OUTSIDE DIMENSION FOR TABLES AND ILLUSTRATIONS
9-1/8"
3/8"

EPA-287 (Cin.)
(4-76)

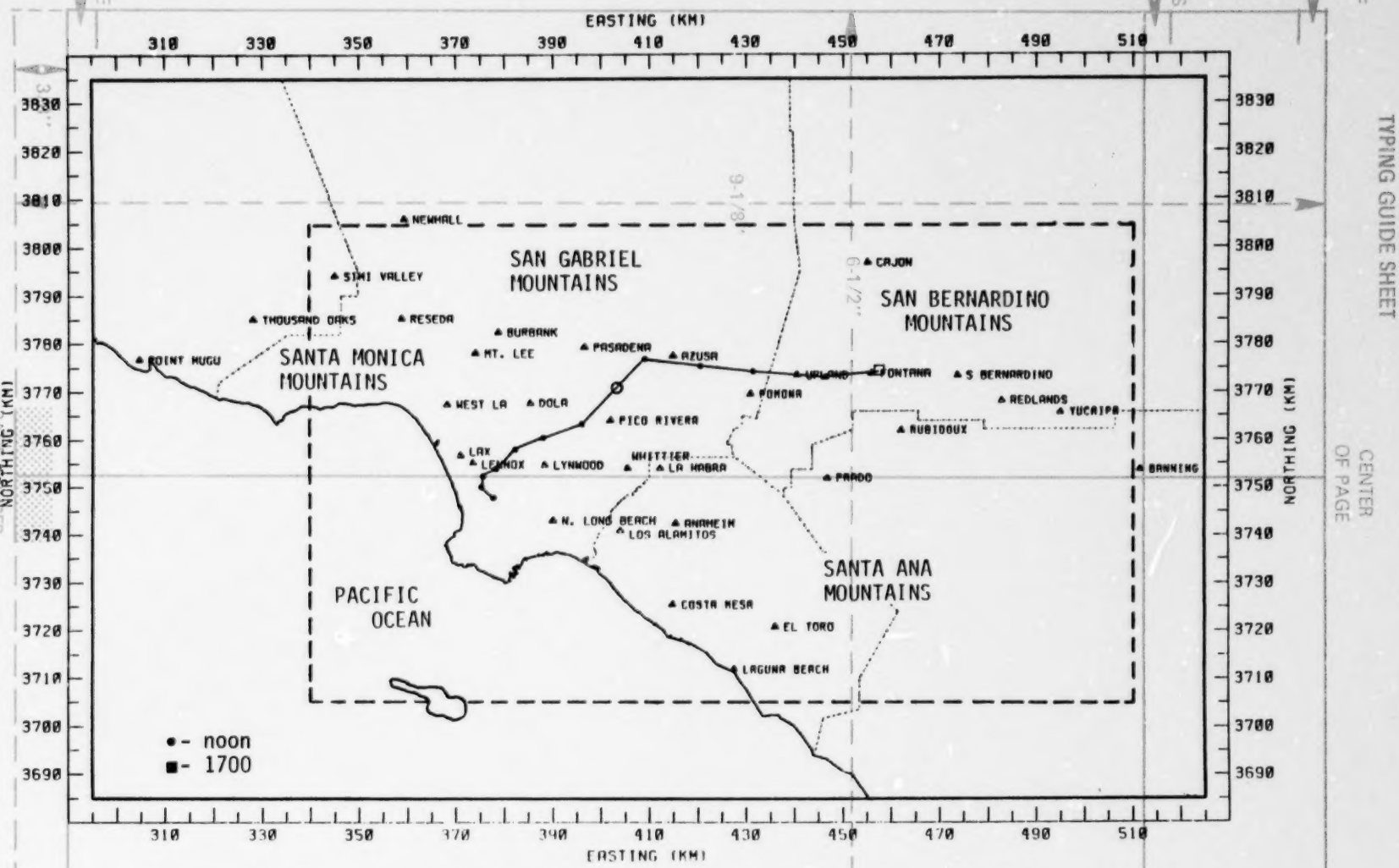

Figure 4. Trajectory of Air parcel on 27 June 1974, at 0500-1700.

BEGIN LAST LINE OF TEXT
DROPPED HEAD; BEGIN SECTIONS HERE
BEGIN FIRST LINE OF TEXT HERE
TYPING GUIDE SHEET
EPA-287 (Cin.) (4-76)
PAGE NUMBER
CENTER OF PAGE
BOTTOM OF IMAGE AREA, OUTSIDE DIMENSION FOR TABLES AND ILLUSTRATIONS
TOP OF IMAGE AREA

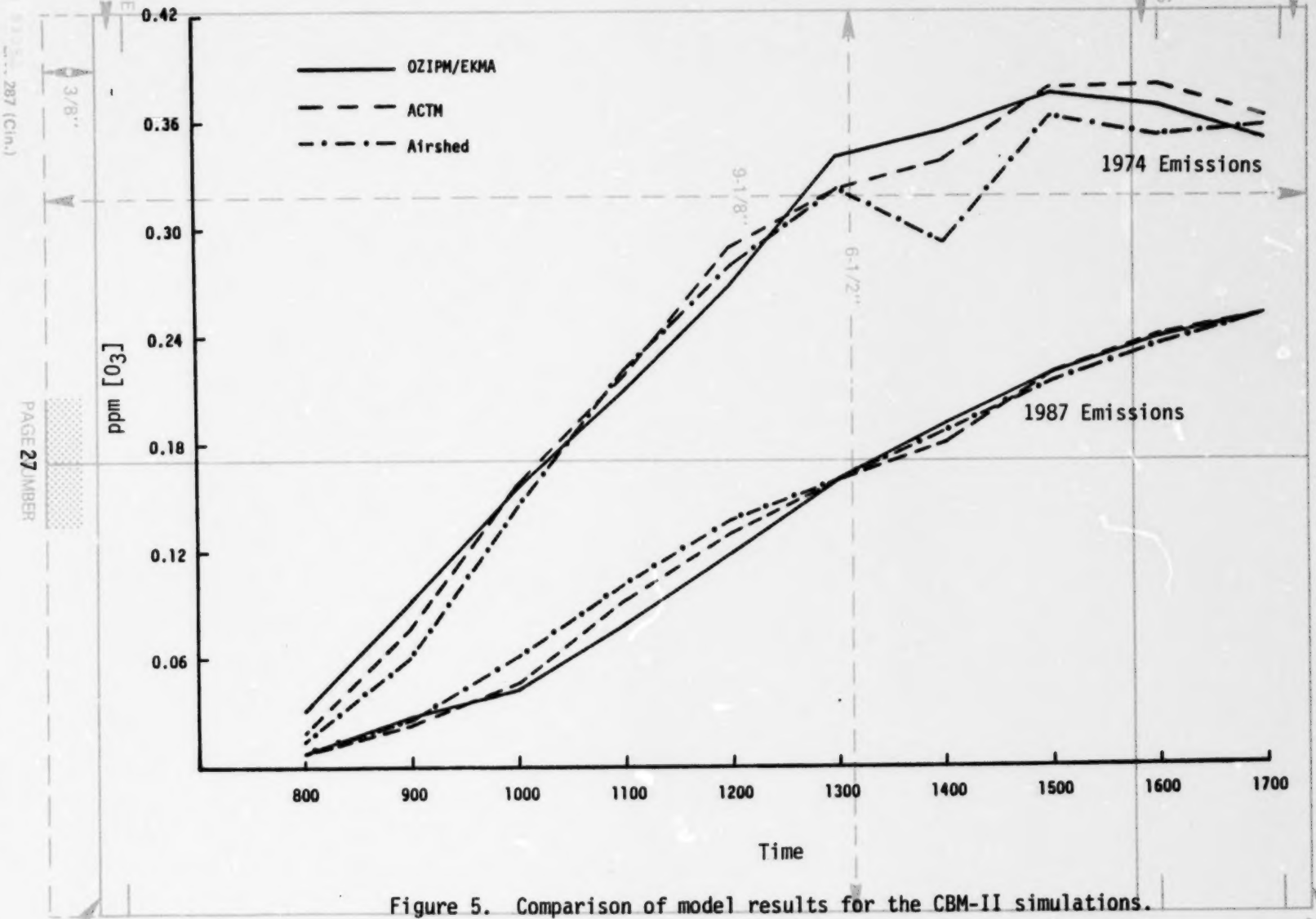

Figure 5. Comparison of model results for the CBM-II simulations.

BEGIN FIRST LINE OF TEXT HERE
TYPING GUIDE SHEET
CENTER OF PAGE
TOP OF IMAGE AREA
DROPPED HEAD; BEGIN SECTIONS HERE

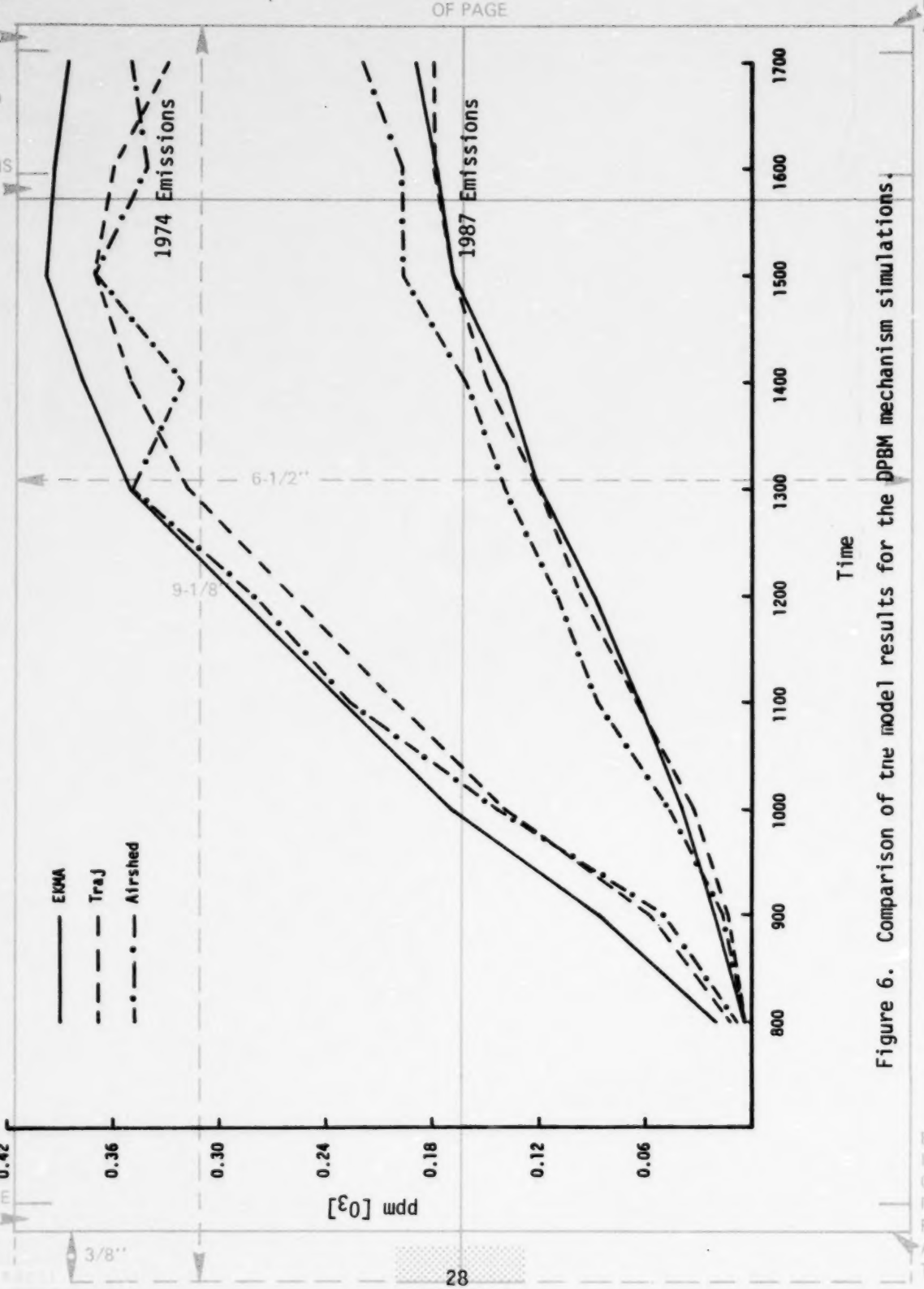

Figure 6. Comparison of the model results for the DPBM mechanism simulations.

BEGIN LAST LINE OF TEXT
3/8"
BOTTOM OF IMAGE AREA; OUTSIDE DIMENSION FOR TABLES AND ILLUSTRATIONS

EPA-287 (Cin.)
(4-76)

BEGIN FIRST LINE OF TEXT HERE
TYPING GUIDE SHEET
CENTER OF PAGE
TOP OF IMAGE AREA
DROPPED HEAD; BEGIN SECTIONS HERE

San Gabriel Mountains, and the Airshed Model predicts high horizontal concentration gradients (≈ 0.01 ppm O_3/km). It is to be expected that the greatest disparity between model calculations would occur under conditions of high wind shear and high concentration gradients, since small differences in the location of the trajectory yield large differences in concentrations.

THE OZIPM/EKMA MODEL

The use of EKMA in the city-specific mode involves trajectory model simulations of an air parcel as it moves through the urban area; the computer package OZIPP is used with the standard (Dodge) chemistry (Whitten and Hogo 1978a), and OZIPM is used when nonstandard kinetics are employed (Whitten and Hogo, 1978b). The OZIPM/EKMA model using CBM kinetics differs from the ACTM in several important respects, which are listed in Table 5. Several of these differences are not important under most circumstances. The number of cells within the mixed layer, for example, is relatively unimportant because the vertical concentration gradients are small. The differences in calculations resulting from the numerical methods employed have been extensively tested and are generally less than 10 percent, and usually less than 5 percent over the range of conditions commonly encountered.

We attempted to match other inputs to the two models as closely as possible, given the differences in formulation. The speciation of emissions input to OZIPM is taken as the average speciation of emissions input to the ACTM. Similarly, though the precise diurnal behavior of photolysis rates differs between the OZIPM/EKMA and the ACTM, the integrated value of photolysis is the same.

Two potentially important phenomena are not normally treated in OZIPM--surface deposition and the chemical reactions of material aloft. We have tested the effects of these two model features and they are often significant (Figure 7). For the purpose of this study, we chose to treat the chemical reactions aloft in the OZIPM/EKMA model by entraining the average concentration of pollutants entrained by the ACTM along its trajectory. However, this procedure presupposes a prior multicell trajectory simulation. Ideally, the capability to treat chemical reactions in material aloft should be included in the EKMA/OZIPM model.

The loss rates of chemical species due to deposition are also difficult to treat. Although it is a simple matter to establish a first-order loss rate for a species in OZIPM (similar to the treatment of chamber wall effects in smog chamber simulations), the loss rate from

BEGIN LAST LINE OF TEXT
BOTTOM OF IMAGE AREA; OUTSIDE DIMENSION FOR TABLES AND ILLUSTRATIONS
3/8"

EPA-287 (Cin.)
(4-76)

BEGIN FIRST LINE OF TEXT HERE
TYPING GUIDE SHEET
CENTER OF PAGE
TOP OF IMAGE AREA
DROPPED HEAD; BEGIN SECTIONS HERE
6-1/2"
9-1/8"
BEGIN LAST LINE OF TEXT
BOTTOM OF IMAGE AREA; OUTSIDE DIMENSION FOR TABLES AND ILLUSTRATIONS
3/8"
PAGE NUMBER
EPA-287 (Cin.) (4-76)

TABLE 5. COMPARISON OF OZIPM AND ACTM TRAJECTORY MODELS

Feature	OZIPM	ACTM
Number of cells	Single cell	Multicell
Material aloft	Kinetic computations not employed	Reacts photochemically
Emission speciation	Constant during run	Temporally and spatially varying
Photolysis rates	Computed interally	Input
Kinetics solution	Gear-Hindemarsh numerical solution	Crank-Nicholson solution; steady-state approximation employed for radical species
Surface deposition	None (may be approximated by first-order decay reactions)	Dependent on surface type and meteorological factors

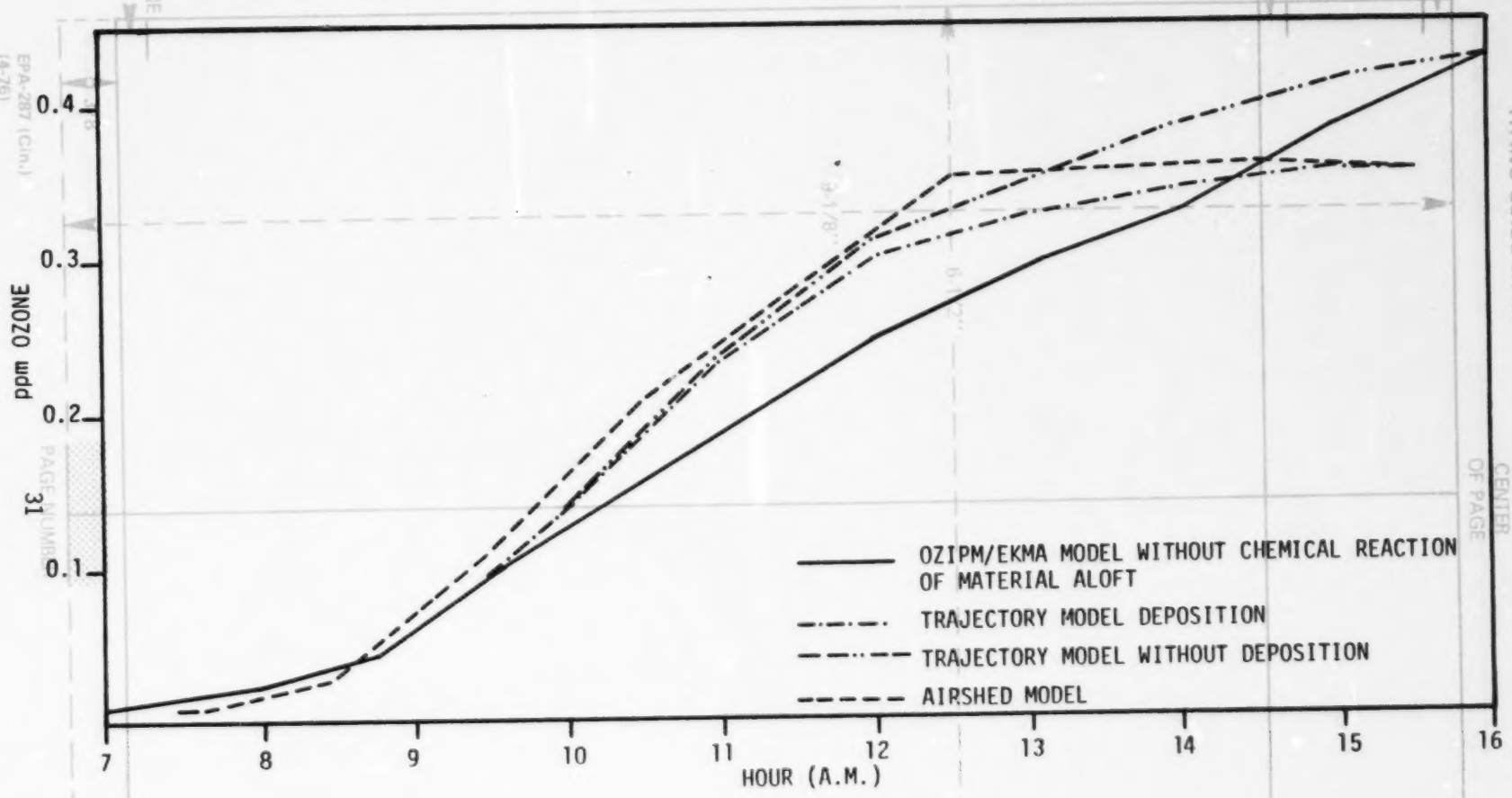

Figure 7. Comparison of model results showing effects of model subcomponents.

BEGIN FIRST LINE OF TEXT HERE
TYPING GUIDE SHEET
CENTER OF PAGE
TOP OF IMAGE AREA
DROPPED HEAD; BEGIN SECTIONS HERE

surface deposition in the ACTM varies greatly because of surface composition and the depth of the mixed layer. (The thickness of the mixed layer determines the surface-to-volume ratio.) In the morning, when the mixed layer is thin and the deposition rate for ozone is rapid, little ozone is available for deposition. In the afternoon, when the ozone level is high, the first-order loss rate is low (see Table 6).

For this reason, simply averaging the first-order loss rate constants is an inappropriate method of treating deposition. Therefore, we averaged only those values occurring after the inversion rise (after 1000 hours). This method yielded a surface loss rate for ozone of 1.5×10^{-3} min^{-1}. The NO_2 surface loss rate was averaged throughout the day using a rate of 4×10^{-3} min^{-1}. Obviously, these numbers are approximations. It is our intention to modify the OZIPM program to treat surface deposition explicitly at some future date.

6-1/2"
9-1/8"
BEGIN LAST LINE OF TEXT
BOTTOM OF IMAGE AREA OUTSIDE DIMENSION FOR TABLES AND ILLUSTRATIONS
3/8"

PAGE NUMBER
EPA-287 (Cin.)
(4-76)

TABLE 6. LOSS RATES OF CHEMICAL SPECIES THROUGH DEPOSITION FOR ACTM
(Fontana trajectory for CBM simulation)

	Ozone			NO_2		
Time	First-order rate constant ($\times 10^3$ min^{-1})	Species concentration (ppm)	Species loss (ppm/min)	First-order rate constant ($\times 10^3$ min^{-1})	Species concentration (ppm)	Species loss (ppm/min)
0500	6.5	2×10^{-4}	1.3×10^{-6}	8.2	0.052	4.3×10^{-4}
0600	6.0	1.1×10^{-3}	6.6×10^{-6}	7.5	0.051	3.8×10^{-4}
0700	5.8	5.9×10^{-3}	3.4×10^{-5}	6.3	0.093	5.8×10^{-4}
0800	8.2	0.019	1.6×10^{-4}	8.8	0.17	1.5×10^{-3}
0900	4.4	0.077	3.4×10^{-4}	5.6	0.15	8.4×10^{-4}
1000	3.7	0.157	5.8×10^{-4}	4.8	0.13	6.2×10^{-4}
1100	1.3	0.22	2.8×10^{-4}	1.8	0.091	1.6×10^{-4}
1200	0.88	0.29	2.5×10^{-4}	1.1	0.07	7.7×10^{-5}
1300	1.4	0.32	4.5×10^{-4}	1.75	0.052	9.1×10^{-5}
1400	1.2	0.34	4.1×10^{-4}	1.5	0.031	4.6×10^{-5}
1500	1.6	0.38	6.1×10^{-4}	2.0	0.026	5.2×10^{-5}
1600	1.2	0.38	4.6×10^{-4}	1.5	0.024	3.6×10^{-5}
1700	1.0	0.36	3.6×10^{-4}	1.3	0.043	5.6×10^{-5}

BEGIN LAST LINE OF TEXT
EPA-287 (Cin.) (4-76)
3/8"
PAGE NUMBER
33
BOTTOM OF IMAGE AREA; OUTSIDE DIMENSION FOR TABLES AND ILLUSTRATIONS
6-1/2"
BEGIN FIRST LINE OF TEXT HERE
DROPPED HEAD; BEGIN SECTIONS HERE
TYPING GUIDE SHEET
CENTER OF PAGE
TOP OF IMAGE AREA

BEGIN FIRST LINE OF TEXT HERE
TYPING GUIDE SHEET
CENTER OF PAGE
TOP OF IMAGE AREA
DROPPED HEAD; BEGIN SECTIONS HERE

SECTION 4

RESULTS AND DISCUSSION

As indicated by the simulation results presented in Figures 5 and 6 and Table 7, we have achieved a reasonable match among the predictions of the Urban Airshed Model, the ACTM, and the OZIPM/EKMA. The computed ozone profiles are somewhat different for simulations using the DPBM Mechanism compared with those using the CBM. For all three models, there is a substantially greater response to the specific control scenario used with the DPBM mechanism than with the CBM. As noted previously, we have traced this greater control response to specific features of the DPBM olefin chemistry, which are discussed in Appendix B.

The effect of mechanism substitution on control strategy predictions is almost the same for both the ACTM and OZIPM/EKMA. For example, in the "peak trajectory" case (Table 8) the O_3 reduction predicted by the ACTM is 34 percent for CBM-II and 51 percent for the DPBM mechanism; for OZIPM/EKMA, the predicted ozone reductions are 33 and 53 percent, respectively. Thus, even though ACTM is more sophisticated than OZIPM, the impact of the two mechanisms on prediction is almost identical; it is less in the Airshed Model, but is still substantial. Ozone reduction predicted for the "peak trajectory" value using the CBM-II is nearly identical for the three models (34, 31, and 33 percent for ACTM, Airshed, and OZIPM/EKMA, respectively). The Airshed Model predicts less control effectiveness with the DPBM mechanism than do the other two models (41 percent for the Airshed Model compared to 51 and 53 percent for the ACTM and OZIPM/EKMA, respectively).

Another phenomenon to contend with concerns the difference in control effectiveness attributable to differences in control criteria (i.e., what ozone concentration value is to be controlled?). The ozone peak measured at a particular station is the value that actually constitutes a violation. For a trajectory model, this corresponds to a specific point along a trajectory. Yet, as Table 8 indicates, one effect of control is to change the timing of the ozone peak. Thus, it is fairly easy to envision a situation in which a control strategy results in attainment at a monitoring site, but in an exceedance downwind of that site.

BEGIN LAST LINE OF TEXT
BOTTOM OF IMAGE AREA OUTSIDE DIMENSION FOR TABLES AND ILLUSTRATIONS
3/8"

PAGE NUMBER
EPA-287 (Cin.) (4-76)

BEGIN FIRST LINE OF TEXT HERE
TYPING GUIDE SHEET
CENTER OF PAGE
TOP OF IMAGE AREA
DROPPED HEAD; BEGIN SECTIONS HERE

TABLE 7. A COMPARISON OF ACTM, AIRSHED, AND OZIPM/EKMA MODEL RESULTS FOR THE FONTANA TRAJECTORY USING THE DPBM AND CARBON-BOND MECHANISM.

	CBM					
	1974			1987		
Time	ACTM	Airshed	OZIPM/EKMA	ACTM	Airshed	OZIPM/EKMA
0800	0.019	0.014	0.029	0.007	0.007	0.011
0900	0.077	0.061	0.092	0.23	0.026	0.029
1000	0.157	0.146	0.158	0.055	0.061	0.052
1100	0.22	0.22	0.21	0.093	0.10	0.081
1200	0.29	0.28	0.27	0.13	0.137	0.12
1300	0.32	0.32	0.34	0.16	0.163	0.16
1400	0.336	0.29	0.354	0.18	0.185	0.19
1500	0.376	0.36	0.375	0.22	0.213	0.22
1600	0.376	0.35	0.367	0.24	0.234	0.24
1700	0.36	0.36	0.358	0.25	0.25	0.25

	DPBM				
1974			1987		
ACTM	Airshed	OZIPM/EKMA	ACTM	Airshed	OZIPM/EKMA
0.01	0.009	0.02			
0.056	0.051	0.086	0.014	0.015	0.021
0.137	0.143	0.17	0.034	0.047	0.039
0.20	0.227	0.23	0.066	0.088	0.064
0.26	0.28	0.29	0.096	0.11	0.09
0.32	0.35	0.35	0.12	0.14	0.12
0.35	0.32	0.368	0.15	0.16	0.14
0.37	0.37	0.398	0.17	0.20	0.17
0.36	0.34	0.394	0.18	0.20	0.18
0.33	0.35	0.386	0.18	0.22	0.19

BEGIN LAST LINE OF TEXT
BOTTOM OF IMAGE AREA; OUTSIDE DIMENSION FOR TABLES AND ILLUSTRATIONS
3/8"
PAGE NUMBER
EPA-287 (Cin.) (4-76)

TABLE 8. EFFECT OF CONTROLS ON ACTM, AIRSHED, AND OZIPM/EKMA MODEL PREDICTIONS FOR THE FONTANA TRAJECTORY

(a) Carbon-Bond Mechanism

Time	1974 Ozone Prediction (ppm)			1987 Ozone Prediction (ppm)			1987/1974 Ratio			Percent O_3 Reduction		
	ACTM	Airshed	OZIPM/EKMA	ACTM	Airshed	OZIPM	ACTM	Airshed	OZIPM/EKMA	ACTM	Airshed	OZIPM/EKMA
1500	0.376	0.36	0.375	0.22	0.21	0.22	0.59	0.58	0.59	41	42	41
1600	0.376	0.35	0.367	0.24	0.234	0.24	0.64	0.67	0.65	36	33	35
1700	0.36	0.36	0.36	0.25	0.25	0.25	0.69	0.69	0.69	31	31	31
Peak trajectory value	0.376	0.36	0.375	0.25	0.25	0.25	0.66	0.69	0.66	34	31	33
Peak value anywhere in Airshed grid		0.39 (at 1700 near Fontana)			0.29 (at 1700 near Fontana)			0.74			26	

(b) DPBM Mechanism

Time	1974 Ozone Prediction (ppm)			1987 Ozone Prediction (ppm)			1987/1974 Ratio			Percent O_3 Reduction		
	ACTM	Airshed	OZIPM/EKMA	ACTM	Airshed	OZIPM/EKMA	ACTM	Airshed	OZIPM	ACTM	Airshed	OZIPM/EKMA
1500	0.37	0.37	0.40	0.17	0.20	0.17	0.46	0.54	0.42	54	46	58
1600	0.36	0.34	0.40	0.18	0.20	0.18	0.30	0.59	0.45	50	41	55
1700	0.33	0.35	0.39	0.18	0.22	0.19	0.54	0.63	0.49	45	37	51
Peak trajectory value	0.37	0.37	0.40	0.18	0.22	0.19	0.49	0.39	0.47	51	41	53
Peak value anywhere in Airshed grid		0.40 (at 1400 near Fontana)			0.24 (at 1600 near Fontana)			0.60			40	

BEGIN FIRST LINE OF TEXT HERE
TYPING GUIDE SHEET
CENTER OF PAGE
TOP OF IMAGE AREA
DROPPED HEAD: BEGIN SECTIONS HERE

Moreover, control calculations obtained using a trajectory model are inherently specific to a particular trajectory. A grid model, however, performs calculations for all possible trajectories simultaneously. The trajectory that reaches the monitored peak value may not be the trajectory that yields the peak ozone value (in either the base year or the projected year), and the peak ozone value predicted for the entire area by the grid model may be higher than the design values for the trajectory model. Thus, the Airshed Model tends to predict a lesser degree of control effectiveness than that predicted by trajectory models.

On the basis of the "grid peak," the control effectiveness for the Airshed CBM-II runs was 26 percent versus 40 percent for the DPBM, a comparison ratio of 65 percent. The "peak trajectory" control effectiveness for OZIPM/EKMA was 33 percent for CBM-II and 53 percent for DPBM, a comparison ratio of 62 percent.

SUMMARY AND CONCLUSIONS

We have performed oxidant air quality base-case and control-scenario simulations for two trajectory models (the DPBM and OZIPM/EKMA models) and a grid model (the Urban Airshed Model) using two different kinetic mechanisms (DPBM and CBM). When the same chemical mechanisms were used, all three models predicted similar amounts of ozone formation and similar responses to the control scenario, provided care was taken to ensure similar simulation conditions (kinetic mechanism, emissions, trajectories, sunlight, deposition, etc.). When different chemical mechanisms were used, the predictions of control-strategy effectiveness were found to vary substantially.

Although trajectory and grid models can show a high degree of similarity in predictions at particular points along a trajectory, or for particular trajectories, a grid model yields information regarding all trajectories in the airshed, including those trajectories that may respond less to control strategies than trajectories examined by a trajectory model. Thus, a primary advantage offered by a grid model is the capability of examining the entire airshed, rather than a limited number of trajectories. Trajectory models, on the other hand, allow an intensive examination of the effects of a particular input variable or model subcomponent (e.g., the kinetic mechanism) at a low cost and with fewer confounding variables than exist in airshed simulations. Therefore, a multimodel approach appears to represent the most efficient analytical procedure for air quality assessment analysis.

BEGIN LAST LINE OF TEXT
BOTTOM OF IMAGE AREA, OUTSIDE DIMENSION FOR TABLES AND ILLUSTRATIONS
3/8"

PAGE NUMBER
EPA-287 (Cin.) (4-76)

BEGIN FIRST LINE OF TEXT HERE
TYPING GUIDE SHEET
CENTER OF PAGE
TOP OF IMAGE AREA
DROPPED HEAD; BEGIN SECTIONS HERE

REFERENCES

Brice, K. A. (1983), "UK Model for Regional Transport of Photochemical Oxidants and Their Precursors," presented at the OECD Conference on Regional Oxidant Transport Modeling, April 12-14, Research Triangle Park, North Carolina.

Dimitriades, B. (1972), "Effects of Hydrocarbon and Nitrogen Oxides on Photochemical Smog Formation," Environ. Sci. Technol., Vol. 6, No. 3, pp. 253-260.

Demerjian, K. L., and K. L. Schere (1979), "Applications of a Photochemical Box Model for Ozone Air Quality in Houston, Texas," In Proc. Ozone/oxidants Interactions with the Total Environment II, Oct. 14-17, Houston, Texas, pp. 414-21.

Dodge, M. C. (1977), "Combined Use of Modeling Techniques and Smog Chamber Data to Derive Ozone-Precursor Relationships," Proc. International Conference on Photochemical Oxidant Pollution and Its Control, EPA-600/3-77-001b, U.S. Environmental Protection Agency, Research Triangle Park, North Carolina.

Dodge, M. C., and R. R. Arnts (1978), "A New Mechanism for the Reaction of Ozone with Olefins," Int. J. Chem. Kinet., Vol. 11, pp. 399-410.

Falls, A. H., and J. H. Seinfeld (1978), "Continued Development of a Kinetic Mechanism for Photochemical Smog," Environ. Sci. Technol., Vol. 12, No. 13, pp. 1398-1406.

Herron, J. T. and R. E. Huie (1977), "Stopped-Flow Studies of the Mechanics of Ozone-Alkene Reactions in the Gas Phase: Ethylene," J. Amer. Chem. Soc., Vol. 99, pp. 5430-5435.

Herron, J. T., R. I. Martinez, and R. E. Huie (1982), "Kinetics and Energetics of the Criegee Intermediate in Ozone-Alkene Reactions," Int. J. Chem. Kinet., Vol. 14, pp. 201-224.

6-1/2"
BEGIN LAST LINE OF TEXT
BOTTOM OF IMAGE AREA OUTSIDE DIMENSION FOR TABLES AND ILLUSTRATIONS
3/8"

PAGE NUMBER
EPA-287 (Cin.) (4-76)

BEGIN FIRST LINE OF TEXT HERE
TYPING GUIDE SHEET
CENTER OF PAGE
TOP OF IMAGE AREA
DROPPED HEAD; BEGIN SECTIONS HERE

Jeffries, H. E., K. G. Sexton, and C. H. Salmi (1981), "Effects of Chemistry and Meteorology on Ozone Control Calculations Using Simple Trajectory Models and the EKMA Procedure," EPA-450/4-81-034, U.S. Environmental Protection Agency, Research Triangle Park, North Carolina.

Killus, J. P., W. R. Oliver, P. D. Gutfreund, J. E. Langstaff, T. W. Tesche, and H. J. Su (1981), "Simulation of Impacts of Nitrogen Oxide Control Strategies under Oxidant Episode Conditions: Vol. 1," Systems Applications, Inc., San Rafael, California.

Lurman, F., D. Godden, C. Lloyd, and R. A. Nordsieck (1979), "A Lagrangian Photochemical Air Quality Simulation Model: Adaptation to the St. Louis-RAPS Data Base--Volume I. Model Formulation," Environmental Research and Technology, Inc., Westlake Village, California.

MacCracken, M. C., and G. D. Sauter, eds. (1975), "Development of an Air Pollution Model for the San Francisco Bay Area," UCRL-51920, Vol. 1, Lawrence Livermore Laboratory, Livermore, California.

McRae, G. J., W. R. Goodin, and J. H. Seinfeld (1982), "Development of a Second-Generation Mathematical Model for Urban Air Pollution: I. Model Formulation," Atmos. Environ., Vol. 16, No. 4, pp. 679-696.

Reynolds, S. D. (1977), "The Systems Applications, Inc. Urban Airshed Model: An Overview of Recent Developmental Work," International Conference on Photochemical Oxidant and Its Control, EPA-600/3-77-001b, Systems Applications, Inc., San Rafael, California.

Reynolds, S. D., L. Reid, M. Hillyer, J. P. Killus, T. W. Tesche, R. I. Pollack, G. E. Anderson, and J. Ames (1979), "Photochemical Modeling of Transportation Control Strategies--Volume I. Model Development, Performance Evaluation, and Strategy Assessment," Systems Applications, Inc., San Rafael, California.

Whitten, G. Z., and H. Hogo (1978a), "User's Manual for Kinetics Model and Ozone Isopleth Plotting Package," U.S. Environmental Protection Agency, Office of Research and Development, Research Triangle Park, North Carolina.

Whitten, G. Z., and H. Hogo (1978b), "User's Manual for Ozone Isopleth Plotting with Optional Mechanisms (OZIPM)," EPA-60018-78-014a, U. S. Environmental Protection Agency, Office of Research and Development, Research Triangle Park, North Carolina.

BEGIN LAST LINE OF TEXT
BOTTOM OF IMAGE AREA, OUTSIDE DIMENSION FOR TABLES AND ILLUSTRATIONS
3/8"

PAGE NUMBER
EPA-287 (Cin.)
(4-76)

BEGIN FIRST LINE OF TEXT HERE
TYPING GUIDE SHEET
CENTER OF PAGE
TOP OF IMAGE AREA
DROPPED HEAD; BEGIN SECTIONS HERE
6-1/2"
9-1/8"
BEGIN LAST LINE OF TEXT
BOTTOM OF IMAGE AREA, OUTSIDE DIMENSION FOR TABLES AND ILLUSTRATIONS
3/8"
PAGE NUMBER
EPA-287 (Cin.)
(4-76)

Whitten, G. Z., J. P. Killus, and H. Hogo (1980), "Modeling of Simulated Photochemical Smog with Kinetic Mechanisms. Vol 1. Final Report," EPA-600/3-80-028a, U.S. Environmental Protection Agency, Office of Research and Development, Research Triangle Park, North Carolina.

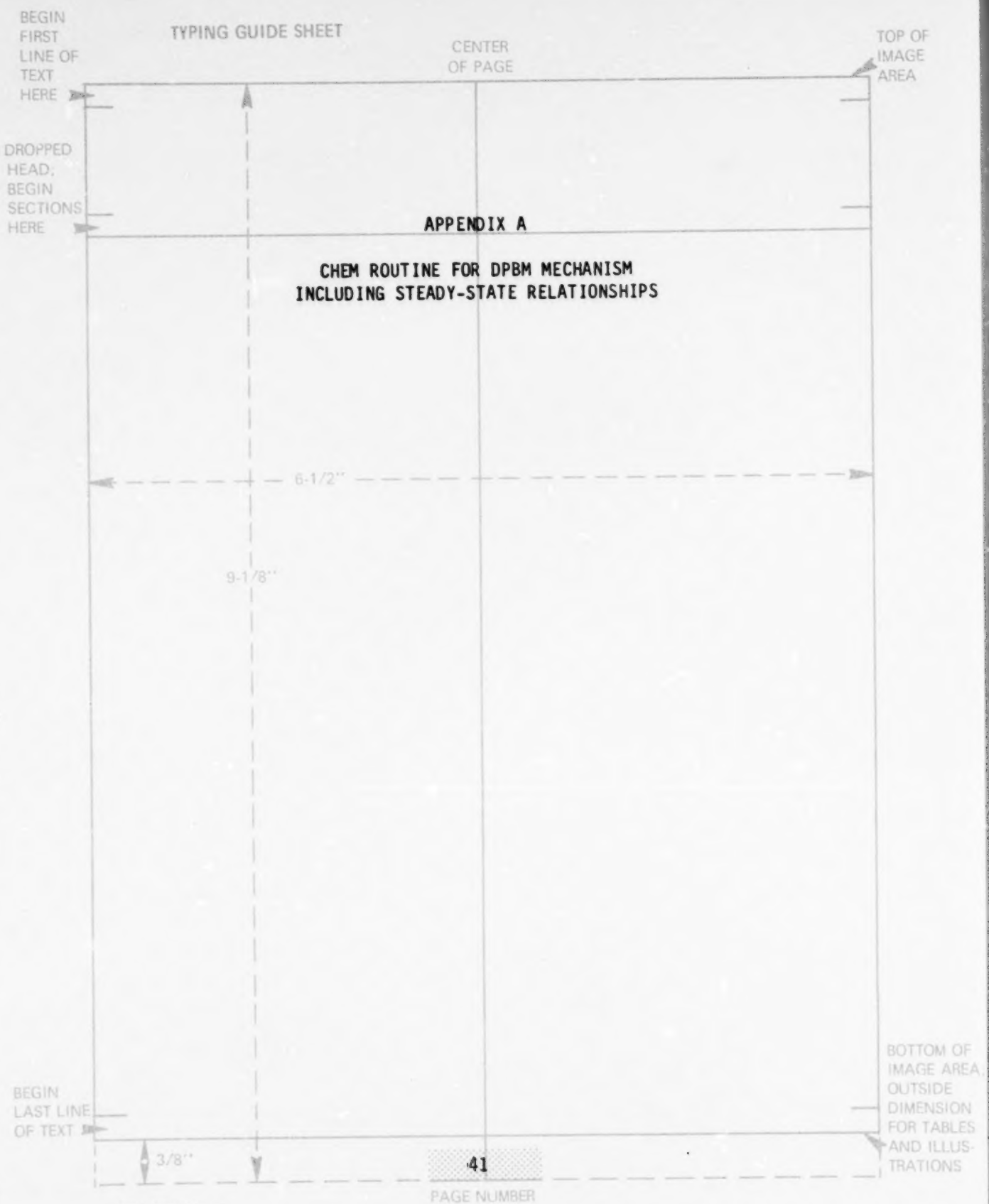
BEGIN FIRST LINE OF TEXT HERE
TYPING GUIDE SHEET
CENTER OF PAGE
TOP OF IMAGE AREA
DROPPED HEAD; BEGIN SECTIONS HERE
APPENDIX A
CHEM ROUTINE FOR DPBM MECHANISM INCLUDING STEADY-STATE RELATIONSHIPS
6-1/2"
9-1/8"
BEGIN LAST LINE OF TEXT
3/8"
BOTTOM OF IMAGE AREA, OUTSIDE DIMENSION FOR TABLES AND ILLUSTRATIONS
41
PAGE NUMBER
EPA-287 (Cin.)
(4-76)

BEGIN FIRST LINE OF TEXT HERE
TYPING GUIDE SHEET
CENTER OF PAGE
TOP OF IMAGE AREA
DROPPED HEAD; BEGIN SECTIONS HERE
6-1/2"
9-1/8"
BOTTOM OF IMAGE AREA; OUTSIDE DIMENSION FOR TABLES AND ILLUSTRATIONS
BEGIN LAST LINE OF TEXT
3/8"

```
      SUBROUTINE CHEM (NOSPEC, NORS, LRADS, HH, H2O,
     $  RATE, R, LERROR)
C
C     KEN DEMERJIAN'S CHEMISTRY
C
C     ***  COMPUTE STEADY-STATE VALUES FOR RADICAL TERMS
C
C     ***  COMPUTE CHEMICAL REACTION RATES FOR EACH SPECIES   (RATE)
C          AND NEGATIVE PARTIAL DERIVATIVES   (R)
C
C     LAST MODIFIED NOV 9, 1982.
C
C--INPUT VARIABLES
C          NOSPEC     I  NO OF SPECIES
C          NORS       I  NO OF REACTIVE SPECIES
C          LRADS      L  RADICALS FLAG--.TRUE.=RADICALS ONLY
C          HH         R  CONCENTRATIONS (PPM)
C          H2O        R  CONCENTRATION OF H2O (PPM)
C
C--OUTPUT VARIABLES
C          RATE       R  RATE FOR EACH SPECIES
C          R          R  NEG PARTIAL DERIV OF EACH RATE W R TO EACH SPEC
C          LERROR     L  .TRUE.=ERROR
C
C--LOCAL VARIABLES
C          SPECIES ARE NAMED FOR READABILITY
C          REACTION RATES ARE OF FORM -RN-
C          INCOMPLETE REACTION TERMS ARE OF FORM -RXN-
C          COEFFICIENTS IN STEADY-STATE EQUATIONS ARE AS DEFINED
C            IN REFERENCE
C
C--ROUTINES CALLED
C          NONE
C
C--CALLED BY
C          STEADY
C          STEP4
C
      LOGICAL LRADS, LERROR
      DIMENSION  HH(NOSPEC)
      DIMENSION  RATE(NORS), R(NORS,NORS)
      REAL NO, NO2, NO3
C
$INSERT EPA1>U_COMDECK>COMDECK.CHDATA
$INSERT EPA1>U_COMDECK>COMDECK.CHPARM
C
C     *** THE FOLLOWING FACTORS ARE FOR CONVERTING PPM TO MICG/CUM
C
CC    DATA  CNIT /2788./
CC    DATA  CORG / 625./
CC    DATA  CSO4 /3948./
C
C
C***********************************************************************
C
C     ***  SET SPECIES-NAMED VARIABLES TO APPROPRIATE VALUES
C
      NO   = HH(KNO   )
      NO2  = HH(KNO2  )
      O3   = HH(KO3   )
      HO4N = HH(KHO4N )
      HNO2 = HH(KHNO2 )
```


EPA-287 (Cin.)
(4-76)

BEGIN FIRST LINE OF TEXT HERE
TYPING GUIDE SHEET
CENTER OF PAGE
TOP OF IMAGE AREA
DROPPED HEAD; BEGIN SECTIONS HERE
9-1/8"
BEGIN LAST LINE OF TEXT
BOTTOM OF IMAGE AREA; OUTSIDE DIMENSION FOR TABLES AND ILLUSTRATIONS
3/8"

```
      OLE  = HH(KOLE )
      PAR  = HH(KPAR )
      ALD = HH(KALD)
      ARO  = HH(KARO )
      PAN  = HH(KPAN )
      CO   = HH(KCO  )
      IF (LSO2) SO2 = HH(KSO2 )
C
C     ***  COMPLETE REACTION TERMS CONTAINING RADICALS
C
CA
C     ***  FOR OXYGEN ATOMS
      O=RK(1)*NO2/(RK(2)+OLE*RK(19))
C
C     ***  FOR OH
      A1=HNO2*RK(7)
      B1=NO*RK(10)+O3*RK(16)
      D1=RK(13)*HNO2+RK(14)*NO2+RK(15)*NO+RK(17)*O3
     $  +RK(21)*OLE+RK(22)*PAR+RK(24)*ALD+RK(32)*ARO
     $  +RK(8)*CO
C
C     ***  FOR RO2
      A2=OLE*O*RK(19)+OLE*O3*RK(20)+0.5*ALD*RK(23)
      B2=RK(21)*OLE+RK(22)*PAR
      D2=NO*RK(25)+O3*RK(29)
C
C     ***  FOR HO2
      A4=HO4N*RK(12)+OLE*O*RK(19)+OLE*O3*RK(20)+1.5*ALD*RK(23)
      B4=CO*RK(8)+O3*RK(17)+RK(24)*0.5*ALD+ARO*RK(32)
      D4=NO2*RK(9)+NO*RK(10)+O3*RK(16)+NO2*RK(11)
C
C     ***  FOR RO
      A3=RK(25)*NO+RK(29)*O3
      D3=RK(26)+RK(28)*NO2
C
C     ***  FOR R1O2
      D5=NO*RK(30)+NO2*RK(27)+O3*RK(36)
C
      SIMP1=NO*RK(30)*PAN*RK(31)*RK(26)
      SIMP2=NO*RK(30)*ALD*RK(24)*RK(26)*0.5
      SIMP3=ARO*RK(32)*D2*D3*D5+RK(26)*A3*B2*D5
     $      +SIMP2*A3+B4*D2*D3*D5
C
      A=RK(18)*D2*D3*D5*D1
      B=D2*D3*D5*D1*D4-A4*D1*D2*D3*D5-B4*B1*D2*D3*D5
     $ -RK(26)*A3*B2*B1*D5-RK(26)*A3*NO*RK(30)*ALD*0.5*RK(24)*B1
      C=-A4*D2*D3*D5*D1-B4*A1*D2*D3*D5-RK(26)*A3*A2*D1*D5
     $ -RK(26)*A3*B2*A1*D5-RK(26)*A3*NO*RK(30)*PAN*RK(31)*D1
     $ -RK(26)*A3*NO*RK(30)*ALD*0.5*RK(24)*A1
C
      A=A*1.0E-15
      B=B*1.0E-15
      C=C*1.0E-15
C
      HO2=-2.*C/(B+SQRT(B**2-4.*A*C))
C
C     ***  FOR OH
      OH=A1/D1+HO2*B1/D1
C
C     ***  FOR R1O2
      R1O2=PAN*RK(31)/D5+0.5*ALD*RK(24)*OH/D5
C
C     ***  FOR RO2
      RO2=A2/D2+OH*B2/D2+R1O2*(NO*RK(30)+O3*RK(36))/D2
```

BEGIN FIRST LINE OF TEXT HERE
TYPING GUIDE SHEET
CENTER OF PAGE
TOP OF IMAGE AREA
DROPPED HEAD; BEGIN SECTIONS HERE
BEGIN LAST LINE OF TEXT
BOTTOM OF IMAGE AREA; OUTSIDE DIMENSION FOR TABLES AND ILLUSTRATIONS
3/8"
PAGE NUMBER
EPA-287 (Cin.) (4-76)

```
C
C     ***  FOR R2O
      R2O=OH*ARO*RK(32)/RK(34)
C
C     ***  FOR RO
      RO=RO2*A3/D3
C
C     ***  FOR NO3
      NO3=O3*NO2*RK(4)/(NO*RK(5)+NO2*RK(6))
      XNO3=NO3
C
C     ***  FOR R2O2
      R2O2=ARO*RK(32)*OH/(RK(33)*NO+RK(35)*O3)
C
CB
      R1=RK(1)*NO2
      R2=RK(2)*O
      R3=RK(3)*O3*NO
      R4=RK(4)*O3*NO2
      R5=RK(5)*NO3*NO
      R6=RK(6)*NO3*NO2
      R7=RK(7)*HNO2
      R8=RK(8)*CO*OH
      R9=RK(9)*HO2*NO2
      R10=RK(10)*HO2*NO
      R11=RK(11)*HO2*NO2
      R12=RK(12)*HO4N
      R13=RK(13)*OH*HNO2
      R14=RK(14)*OH*NO2
      R15=RK(15)*OH*NO
      R16=RK(16)*O3*HO2
      R17=RK(17)*O3*OH
      R18=RK(18)*HO2*HO2
      R19=RK(19)*OLE*O
      R20=RK(20)*OLE*O3
      R21=RK(21)*OLE*OH
      R22=RK(22)*PAR*OH
      R23=RK(23)*ALD
      R24=RK(24)*ALD*OH
      R25=RK(25)*RO2*NO
      R26=RK(26)*RO
      R27=RK(27)*R1O2*NO2
      R28=RK(28)*RO*NO2
      R29=RK(29)*RO2*O3
      R30=RK(30)*R1O2*NO
      R31=RK(31)*PAN
      R32=RK(32)*ARO*OH
      R33=RK(33)*R2O2*NO
      R34=RK(34)*R2O
      R35=RK(35)*R2O2*O3
      R36=RK(36)*R1O2*O3
C
C     ***  COMPUTE DERIVATIVE OF EACH SPECIES I W.R.T. TIME: RATE(I)
C     ***  AND NEGATIVE PARTIAL DERIVATIVE OF EACH RATE I TO
C     ***  EACH SPECIES J: R(I,J)
C
      RNEG=(R3+R5+R10+R15+R25+R28+R30+R33)
      RATE(KNO)=R1+R7-RNEG
      R(KNO,KNO)=RNEG/NO
      R(KNO,KNO2)=-R1/NO2
      R(KNO,KO3)=R3/O3
      R(KNO,KHNO2)=-R7/HNO2
C
      RNEG=R1+R4+R6+R9+R11+R14+R27+R28
```

BEGIN FIRST LINE OF TEXT HERE
TYPING GUIDE SHEET
CENTER OF PAGE
TOP OF IMAGE AREA
DROPPED HEAD; BEGIN SECTIONS HERE

```
      RPOS=R3+2*R5+R18+R25+R38+R33
      RATE(KNO2)=RPOS+R12+R13+R31-RNEG
      R(KNO2,KNO)=-RPOS/NO
      R(KNO2,KNO2)=RNEG/NO2
      R(KNO2,KO3)=-(R3-R4)/O3
      R(KNO2,KHNO2)=-R13/HNO2
      R(KNO2,KHO4N)=-R11/HO4N
      R(KNO2,KPAN)=-R27/PAN
C
      RNEG=R3+R4+R16+R17+R28+R29+R35+R36
      RATE(KO3)=R2-RNEG
      R(KO3,KNO)=R3/NO
      R(KO3,KNO2)=R4/NO2
      R(KO3,KO3)=RNEG/O3
      R(KO3,KOLE)=R28/OLE
C
      RATE(KHNO2)=R9+R16-R7-R13
      R(KHNO2,KNO)=-R15/NO
      R(KHNO2,KNO2)=-(R13-R9)/NO2
      R(KHNO2,KHNO2)=(R7+R13)/HNO2
C
      RATE(KHO4N)=R11-R12
      R(KHO4N,KNO2)=-R11/NO2
      R(KHO4N,KHO4N)=RK(12)
C
      RATE(KOLE)=-R19-R28-R21
      R(KOLE,KO3)=R28/O3
      R(KOLE,KOLE)=-RATE(KOLE)/OLE
C
      RATE(KPAR)=-R22
      R(KPAR,KPAR)=R22/PAR
C
      RATE(KALD)=R19+R28+R21-R23-R24+R26+R32+R34
      R(KALD,KO3)=-R28/O3
      R(KALD,KOLE)=-R28/OLE
      R(KALD,KALD)=(R23+R24)/ALD
C
      RATE(KARO)=-R32
      R(KARO,KARO)=R32/ARO
C
      RATE(KPAN)=R27-R31
      R(KPAN,KNO2)=-R27/NO2
      R(KPAN,KPAN)=RK(31)
C
C
C--COMPUTE RATES FOR SO2 ONLY IF REACTIVE
      IF (.NOT.LSO2) GO TO 688
      RX66 = RK(66) * SO2
      RX69 = RK(69) * SO2
      R66 = RX66 * OH
      R69 = RX69
      RATE(KSO2 ) = -R66 - R69
      R(KSO2,KSO2) = RATE(KSO2) / SO2
  688 CONTINUE
C
C     WRITE(1,1889)
1889  FORMAT('C')
C     WRITE(6,1882)
C     WRITE(6,1883) O,HO2,OH,RIO2,RO2,R2O,RO,NO3,R2O2
1882  FORMAT(1H1//18X,'STEADY STATE CALCULATIONS')
1883  FORMAT(/18X,1PE12.2,3X,'O'
     $ //18X,1PE12.2,3X,'HO2'
     $ //18X,1PE12.2,3X,'OH'
     $ //18X,1PE12.2,3X,'RIO2'
     $ //18X,1PE12.2,3X,'RO2'
     $ //18X,1PE12.2,3X,'R2O'
     $ //18X,1PE12.2,3X,'RO'
     $ //18X,1PE12.2,3X,'NO3'
     $ //18X,1PE12.2,3X,'R2O2')
      RETURN
      END
```

BEGIN LAST LINE OF TEXT
BOTTOM OF IMAGE AREA, OUTSIDE DIMENSION FOR TABLES AND ILLUSTRATIONS
3/8"

EPA-287 (Cin.)
(4-76)

BEGIN FIRST LINE OF TEXT HERE
TYPING GUIDE SHEET
CENTER OF PAGE
TOP OF IMAGE AREA
DROPPED HEAD: BEGIN SECTIONS HERE
APPENDIX B
TESTS OF THE DEMERJIAN PHOTOCHEMICAL BOX MODEL (DPBM) MECHANISM USING SMOG CHAMBER DATA
6-1/2"
9-1/8"
BEGIN LAST LINE OF TEXT
3/8"
BOTTOM OF IMAGE AREA. OUTSIDE DIMENSION FOR TABLES AND ILLUSTRATIONS
46
PAGE NUMBER
EPA-287 (Cin.) (4-76)

BEGIN FIRST LINE OF TEXT HERE
TYPING GUIDE SHEET
CENTER OF PAGE
TOP OF IMAGE AREA
DROPPED HEAD; BEGIN SECTIONS HERE

APPENDIX B

TESTS OF THE DEMERJIAN PHOTOCHEMICAL BOX MODEL (DPBM) MECHANISM USING SMOG CHAMBER DATA

As part of the procedures for implementing and testing the steady-state algorithm and finite-difference solution for the Demerjian Photochemical Box Model (DPBM) Mechanism, we tested the mechanism using several sets of smog chamber data previously used to validate the Carbon-Bond Mechanism (CBM) The data sets used included seven compoent runs from the University of California at Riverside (UCR), and an experiment conducted at the University of North Carolina (UNC) outdoor smog chamber using a synthetic urban mix. We were not able to validate the DPBM mechanism with these experiments. This failure may be traced to two questionable mechanism components whose effects are additive.

The first problem component concerns Reaction 20 (Table 1), in which the reaction of ozone with olefins yields two peroxy radicals. This assumption represents a large net source of hydrogen-containing radicals in the kinetic system. Recent studies of the ozone-olefin reaction using the mechanism of Crigee intermediates (Herron et al., 1982) suggest that the net yield of hydrogen-containing radicals is small and rather complicated. Ethene has been estimated to have an upper limit free radical yield of 9 percent (Herron and Huie, 1977).

The second problem with the DPBM mechanism is found in the lumping scheme. Ethene is treated as an olefin (which is correct) having a reaction rate with O, OH, and O_3 similar to that of propene (which is not correct). The difference in rate constants between propene and ethene is 3:1 for OH, 7:1 for O_3, and 9:1 for O atoms.

These two problems cause a substantial overprediction of the reactivity of olefinic hydrocarbons, since ethene is the major olefin in most simulations. Jeffries et al. (1981) validated the DPBM mechanism using the Bureau of Mines auto exhaust experiments, which had an olefin-carbon mole fraction of 17 percent and an average carbon number of 3, with ethene representing 41 percent of olefinic carbon. In the UNC outdoor smog chamber experiment, the synthetic urban mix had a olefin-carbon mole fraction of 30 percent, with ethene representing 60 percent of olefinic carbon. The excess

BEGIN LAST LINE OF TEXT
BOTTOM OF IMAGE AREA; OUTSIDE DIMENSION FOR TABLES AND ILLUSTRATIONS
3/8"

PAGE NUMBER
EPA-287 (Cin.)
(4-76)

BEGIN FIRST LINE OF TEXT HERE
TYPING GUIDE SHEET
CENTER OF PAGE
TOP OF IMAGE AREA
DROPPED HEAD; BEGIN SECTIONS HERE

radical production predicted using the DPBM mechanism for this speciation is such that aldehyde photolysis may be completely neglected in the simulations; radical initiation from the O atom-olefin reaction and the O_3-olefin reaction will still drive the system more rapidly than has been experimentally observed (Figure B-1).

In the UCR chamber studies (Figures B-2 through B-4), even for those experiments using mixture A (the lowest olefin-carbon mole fraction), the DPBM mechanism still overpredicts the reactivity of the system, with no aldehyde photolysis and no initial HONO. Characteristically, in EC-246 (Figure B-2), the simulated reaction begins slowly, with a time to NO/NO_2 crossover that is late by a factor of 2. However, as soon as the ozone-olefin reaction begins to become effective, predicted O_3 buildup is very rapid and the simulated ozone peak occurs nearly two hours too soon.

On the basis of these results, we conclude that the DPBM mechanism is overly sensitive to the olefin fraction of the hydrocarbon mix, especially when the olefin is ethene. We would recommend either that ethene be treated separately (as in the Carbon-Bond and CIT mechanisms), or that the rate constants for olefins be a weighted average dependent upon olefin speciation. We would also recommend that the radical yield from the ozone-olefin reaction be reduced to be more in keeping with recent work in ozone-olefin chemistry.

BEGIN LAST LINE OF TEXT
BOTTOM OF IMAGE AREA; OUTSIDE DIMENSION FOR TABLES AND ILLUSTRATIONS
3/8"

EPA-287 (Cin.)
(4-76)

BEGIN FIRST LINE OF TEXT HERE
TYPING GUIDE SHEET
CENTER OF PAGE
TOP OF IMAGE AREA
DROPPED HEAD; BEGIN SECTIONS HERE

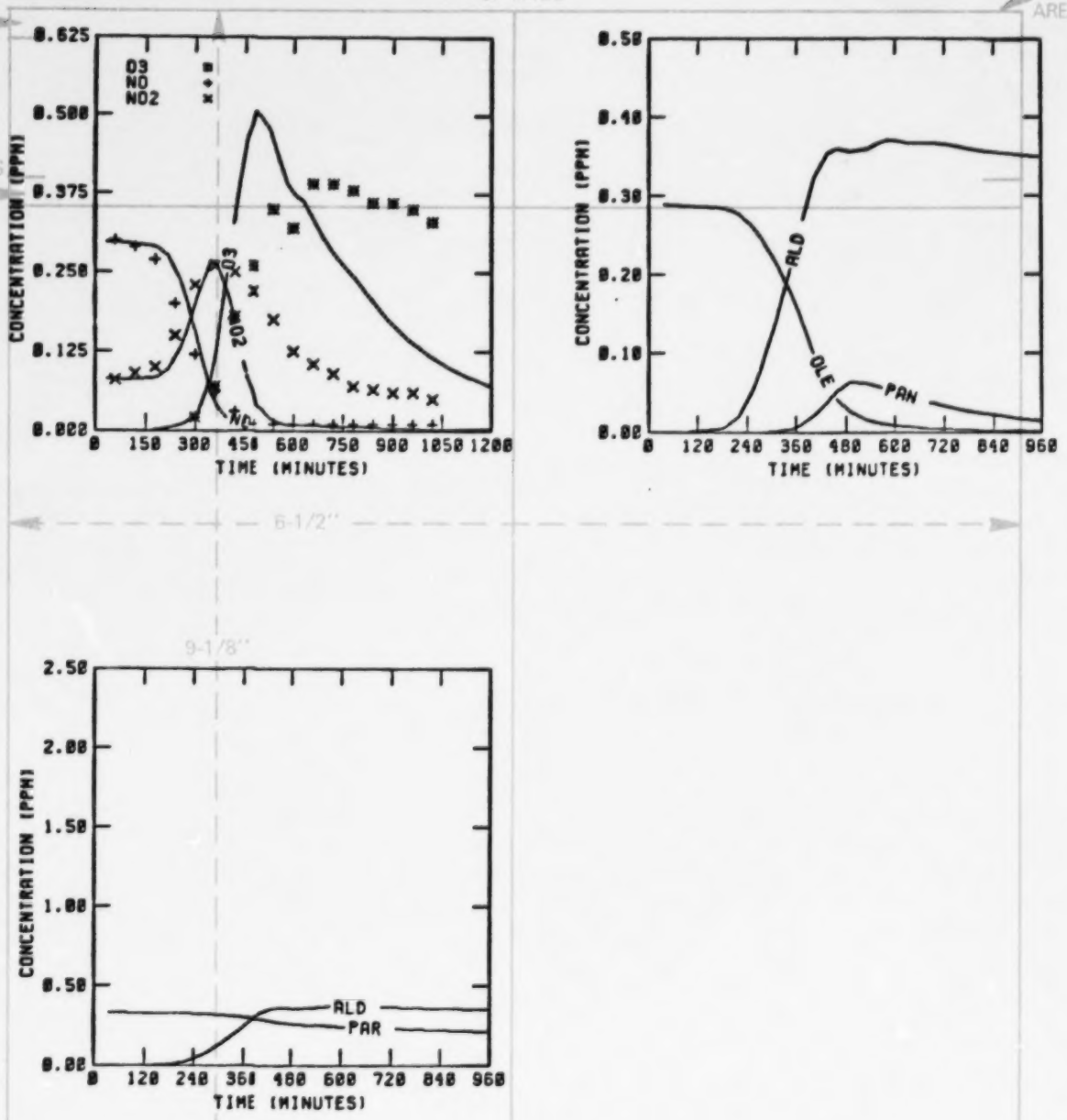

6-1/2"

9-1/8"

FIGURE B-1. UNC Simulation Results for 13 June 1974.

BEGIN LAST LINE OF TEXT
BOTTOM OF IMAGE AREA. OUTSIDE DIMENSION FOR TABLES AND ILLUSTRATIONS
3/8"

EPA-287 (Cin.)
(4-76)

BEGIN FIRST LINE OF TEXT HERE
TYPING GUIDE SHEET
CENTER OF PAGE
TOP OF IMAGE AREA
DROPPED HEAD; BEGIN SECTIONS HERE

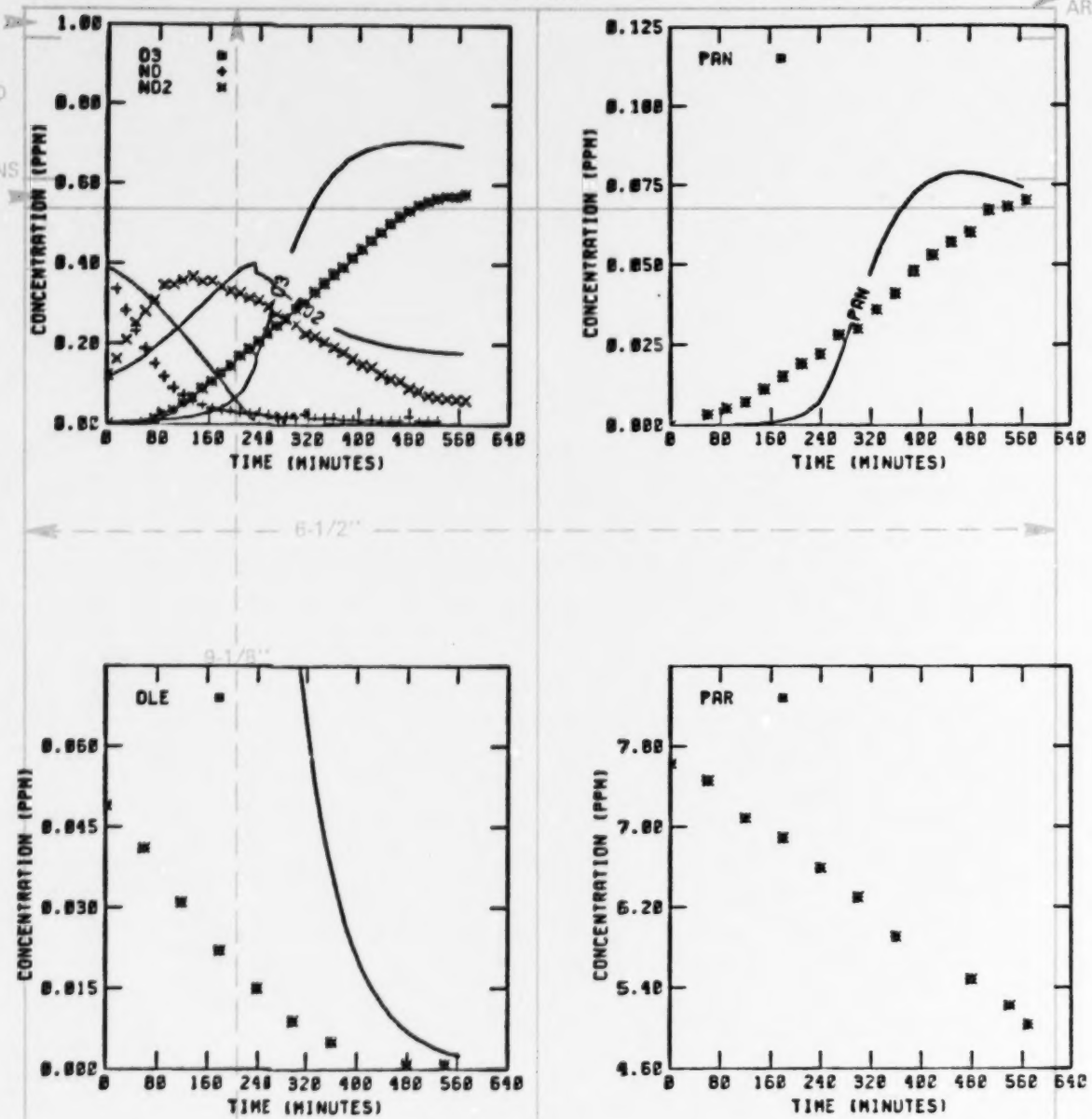

6-1/2"
9-1/8"

FIGURE B-2. UCR Simulation Results for EC-246.

BEGIN LAST LINE OF TEXT
BOTTOM OF IMAGE AREA, OUTSIDE DIMENSION FOR TABLES AND ILLUSTRATIONS
3/8"

EPA-287 (Cln.)
(4-76)

BEGIN FIRST LINE OF TEXT HERE
TYPING GUIDE SHEET
CENTER OF PAGE
TOP OF IMAGE AREA
DROPPED HEAD; BEGIN SECTIONS HERE
6-1/2"
9-1/8"
BEGIN LAST LINE OF TEXT
3/8"
BOTTOM OF IMAGE AREA, OUTSIDE DIMENSION FOR TABLES AND ILLUSTRATIONS
PAGE NUMBER
EPA-287 (Cin.) (4-76)

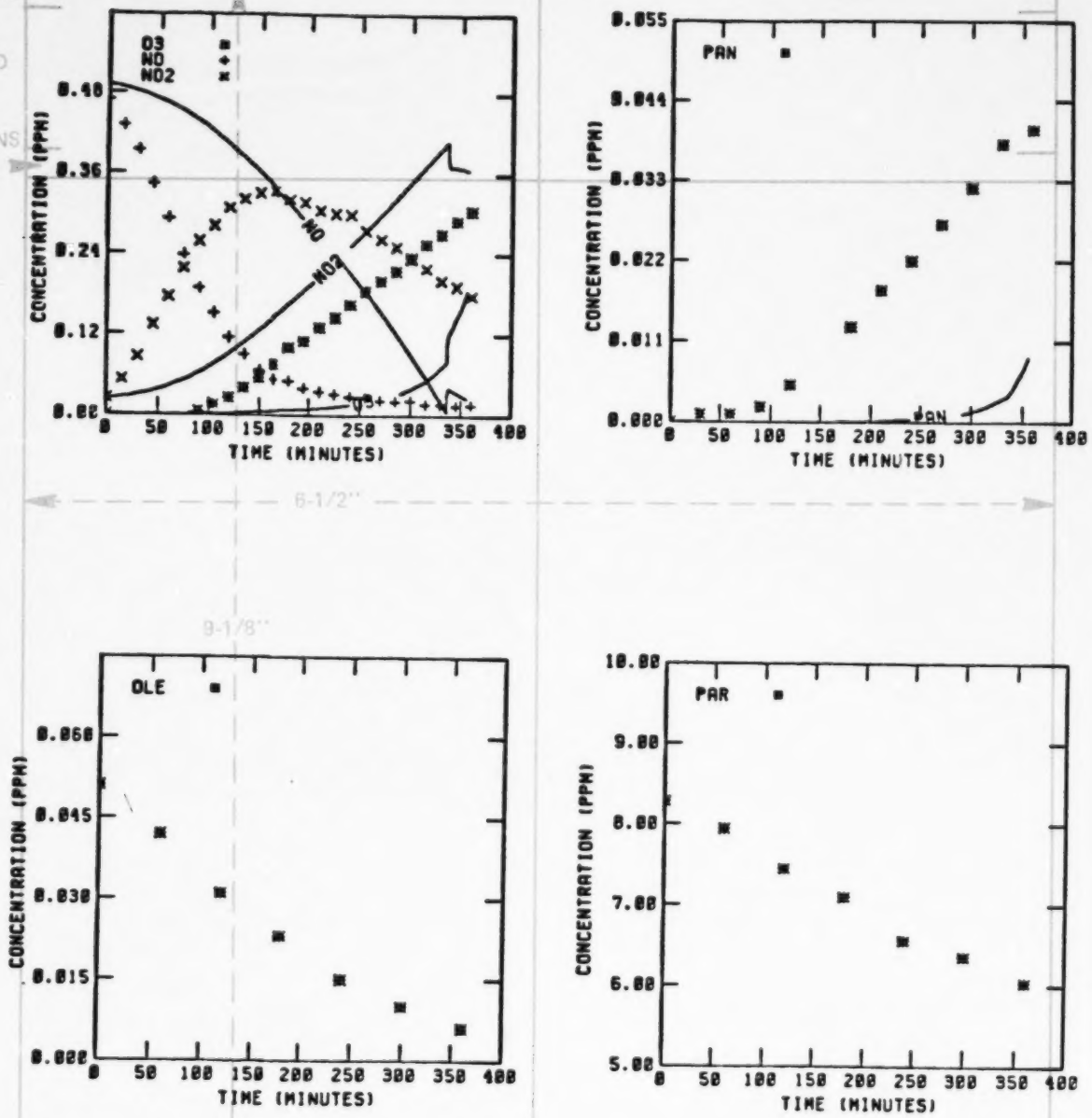

FIGURE B-3. UCR Simulation Results for EC-232.

BEGIN FIRST LINE OF TEXT HERE
TYPING GUIDE SHEET
CENTER OF PAGE
TOP OF IMAGE AREA
DROPPED HEAD; BEGIN SECTIONS HERE

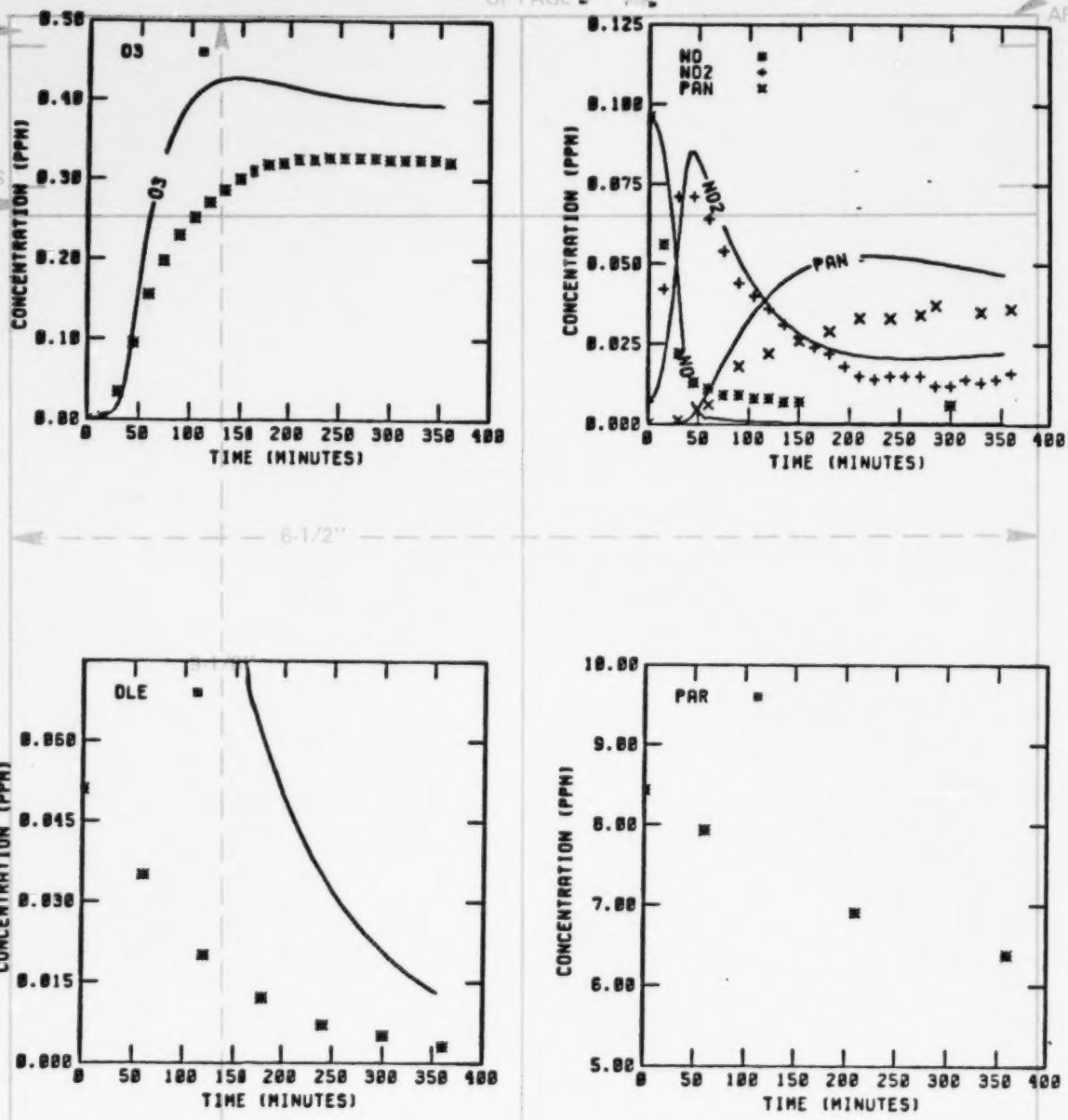

6-1/2"

FIGURE B-4. UCR Simulation Results for EC-233.

BEGIN LAST LINE OF TEXT
BOTTOM OF IMAGE AREA; OUTSIDE DIMENSION FOR TABLES AND ILLUSTRATIONS
3/8"

EPA-287 (Cin.)
(4-76)